

Cite this: *Biomater. Sci.*, 2021, **9**, 6337

# Exploiting the role of nanoparticles for use in hydrogel-based bioprinting applications: concept, design, and recent advances

Aishik Chakraborty,<sup>a</sup> Avinava Roy,<sup>b</sup> Shruthi Polla Ravi<sup>c</sup> and Arghya Paul \*<sup>d</sup>

Three-dimensional (3D) bioprinting is an emerging tissue engineering approach that aims to develop cell or biomolecule-laden, complex polymeric scaffolds with high precision, using hydrogel-based “bioinks”. Hydrogels are water-swollen, highly crosslinked polymer networks that are soft, quasi-solid, and can support and protect biological materials. However, traditional hydrogels have weak mechanical properties and cannot retain complex structures. They must be reinforced with physical and chemical manipulations to produce a mechanically resilient bioink. Over the past few years, we have witnessed an increased use of nanoparticles and biological moiety-functionalized nanoparticles to fabricate new bioinks. Nanoparticles of varied size, shape, and surface chemistries can provide a unique solution to this problem primarily because of three reasons: (a) nanoparticles can mechanically reinforce hydrogels through physical and chemical interactions. This can favorably influence the bioink’s 3D printability and structural integrity by modulating its rheological, biomechanical, and biochemical properties, allowing greater flexibility to print a wide range of structures; (b) nanoparticles can introduce new bio-functionalities to the hydrogels, which is a key metric of a bioink’s performance, influencing both cell–material and cell–cell interactions within the hydrogel; (c) nanoparticles can impart “smart” features to the bioink, making the tissue constructs responsive to external stimuli. Responsiveness of the hydrogel to magnetic field, electric field, pH changes, and near-infrared light can be made possible by the incorporation of nanoparticles. Additionally, bioink polymeric networks with nanoparticles can undergo advanced chemical crosslinking, allowing greater flexibility to print structures with varied biomechanical properties. Taken together, the unique properties of various nanoparticles can help bioprint intricate constructs, bringing the process one step closer to complex tissue structure and organ printing. In this review, we explore the design principles and multifunctional properties of various nanomaterials and nanocomposite hydrogels for potential, primarily extrusion-based bioprinting applications. We illustrate the significance of biocompatibility of the designed nanocomposite hydrogel-based bioink for clinical translation and discuss the different parameters that affect cell fate after cell–nanomaterial interaction. Finally, we critically assess the current challenges of nanoengineering bioinks and provide insight into the future directions of potential hydrogel bioinks in the rapidly evolving field of bioprinting.

Received 18th April 2021,  
Accepted 24th July 2021  
DOI: 10.1039/d1bm00605c  
rsc.li/biomaterials-science<sup>a</sup>Department of Chemical and Biochemical Engineering, The University of Western Ontario, London, ON N6A 5B9, Canada<sup>b</sup>Metallurgy and Materials Engineering, Indian Institute of Engineering Science and Technology, Shibpur, West Bengal 711103, India<sup>c</sup>School of Biomedical Engineering, The University of Western Ontario, London, ON N6A 5B9, Canada<sup>d</sup>Department of Chemical and Biochemical Engineering, Department of Chemistry, School of Biomedical Engineering, The University of Western Ontario, London, ON N6A 5B9, Canada. E-mail: arghya.paul@uwo.ca

## 1. Introduction

Three-dimensional (3D) bioprinting is an innovative method of artificially fabricating tissues and organs by spatially distributing living cells with or without supporting materials in the form of biopolymers and biologics.<sup>1–4</sup> This computer-guided, robotic, layer-by-layer cell and/or biomaterial deposition strategy helps in constructing complex tissue microstructures and fabricating tissue engineered organs to meet global organ shortage. Bioprinted *in vitro* tissue models can also be used for testing drug candidates and has the potential to minimize preclinical animal testing needs. Other than the *in vitro* development of 3D constructs, 3D bioprinting can be used during

ongoing surgeries under clinical settings.<sup>5</sup> This fascinating, intraoperative, real-time *in vivo* approach involves the printing of tissue mimics directly at the location of the injury. However, for safe and effective biomedical applications of 3D bioprinting technology, fundamental knowledge of the material properties to be printed (also known as “biomaterial ink”) is very crucial. The materials to be printed must be injectable, biocompatible, cell-friendly, and biodegradable.<sup>6</sup> The biomaterial ink together with cells are referred to as “bioinks”.<sup>7–10</sup> The cellular component of the bioink severely limits the 3D bioprinting process. Therefore, the ink must be carefully evaluated to fit the demanding process conditions.

Among the different types of materials, hydrogels have been suitably used as bioinks for extrusion-based tissue printing applications.<sup>11–13</sup> Hydrogels are water-retaining, crosslinked, polymeric chains that closely resemble macromolecular-based structures in the body.<sup>14–16</sup> Hydrogels are excellent candidates for biomedical applications, including 3D bioprinting, because of their bio-friendly material properties.<sup>17</sup> Biopolymers, such as polysaccharides and polypeptides, derived from plant and animal sources are crosslinked either physically or chemically to form natural hydrogels.<sup>18</sup> Natural hydrogels are easily degradable and form desirable scaffolds for cell encapsulation and adhesion. Because of these favorable biological properties, natural polymer-based hydrogels are often selected for 3D bioprinting.<sup>19</sup> However, hydrogels made from purely natural polymers find limited applications.<sup>20</sup> Hydrogels originating from natural sources like gelatin, sodium alginate and chitosan exhibit inferior mechanical pro-

erties. This is particularly problematic for *in vivo* tissue engineering applications. Premature wearing-out of hydrogels can lead to the early degradation of the scaffold and unnecessary formation of cracks at the site of application. Degraded scaffolds can even fall prey to harmful opportunistic microorganisms.<sup>21</sup> Different strategies to modify the polymer chemistry and enhance the applicability of such materials have been investigated over the past decade. Some of the examples include the use of double-network hydrogels,<sup>22</sup> multi-network hydrogels,<sup>23</sup> click chemistry-based hydrogels,<sup>24</sup> and supramolecular hydrogels.<sup>25</sup> However, they are currently limited by one or more of the following parameters – mechanical resilience, printability, shape fidelity, proper mechanical energy dissipation mechanism, biocompatibility, cell-instructive, or biofunctional properties.

Introducing nanoparticles into the polymeric network of hydrogels (also known as nanocomposite hydrogels) has the potential to address the current drawbacks of conventional bioinks.<sup>26,27</sup> In fact, reinforcing hydrogels with nanoparticles can offer unique advantages over earlier discussed strategies.<sup>28</sup> Fig. 1 summarizes some of the crucial functionalities that can be imparted by the appropriate use of nanoparticles. The figure also highlights some possible areas of application of these bioinks. Unique properties, such as photo-responsiveness,<sup>29</sup> magnetic field-responsiveness,<sup>30</sup> and so on, can be integrated by functionalizing the hydrogels with nanoparticles. Different types of nanomaterials are being considered for the functionalization process. For example, carbon-based nanomaterials, such as carbon nanotubes and carbon dots, can

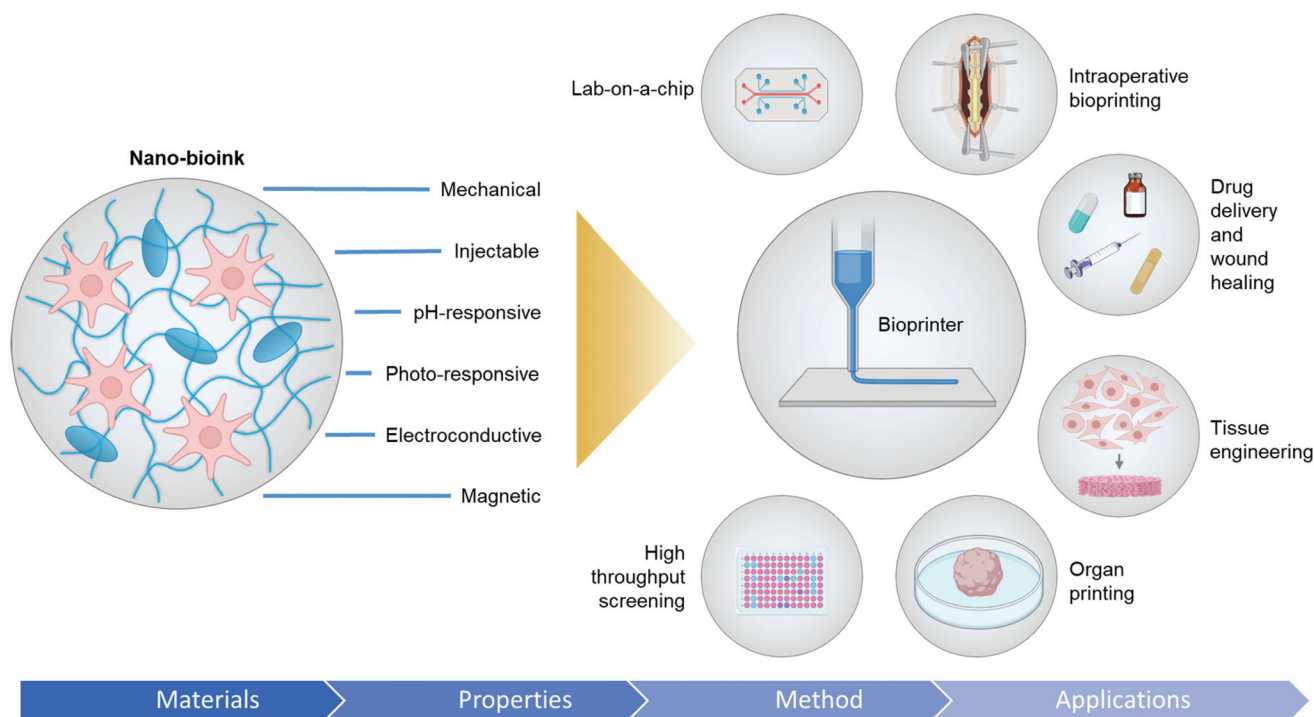


**Fig. 1** Multifunctionalities of nanocomposite hydrogel-based bioinks. Schematic highlights the different functionalities of a bioink imparted by nanoparticles. It also demonstrates the possible applications of nanocomposite hydrogel-based bioinks.

make hydrogels electroconductive, thermally conductive, optically active, and mechanically strong.<sup>31,32</sup> Bioactive inorganic nanoparticles have also been studied for designing nanocomposite hydrogels. Inorganic materials like silicon, calcium, magnesium, and many more, are essential to the proper functioning of the body.<sup>33</sup> Nanoparticles synthesized with these minerals can impart properties unique to such nanomaterials. For instance, nanosilicates, also known as nanoclay/LAPONITE® silicate nanoplatelets, can be added to hydrogels to introduce osteogenic properties.<sup>34</sup> Nanosilicates can also enhance the mechanical properties of hydrogels and help in modulating the release of drugs.<sup>35,36</sup> Metal and metal oxide nanoparticles are also commonly used for fabricating nanocomposite hydrogels.<sup>37</sup> Silver-based nanoparticles show antimicrobial properties that are often used to design nanocomposite hydrogels to counter antibiotic-resistant bacteria.<sup>38</sup> Gold nanospheres can introduce photothermal-responsiveness

in hydrogels.<sup>39</sup> These unique nanocomposite hydrogels are being implemented as drug delivery devices, biosensors, bioactuators, tissue engineering scaffolds and so on. An emerging application of these materials is in the field of 3D bioprinting where they serve as the bioinks.<sup>26,40,41</sup> Fig. 2A–D display injectable nanocomposite hydrogels that have the potential to become bioinks.<sup>36,42–44</sup> However, it should be noted that there are strict process requirements for 3D bioprinting, which will be discussed in section 2. The examples presented in Fig. 2 can become biomaterial inks only when such rigorous process standards are met. In this review, we will focus primarily on the material properties of different nanocomposite hydrogels that are essential to generate the next generation of biomaterial inks and/or bioinks for diverse biomedical applications. Additionally, the review will also provide an insight into the future of these newly formulated bioinks and nanocomposite hydrogels.

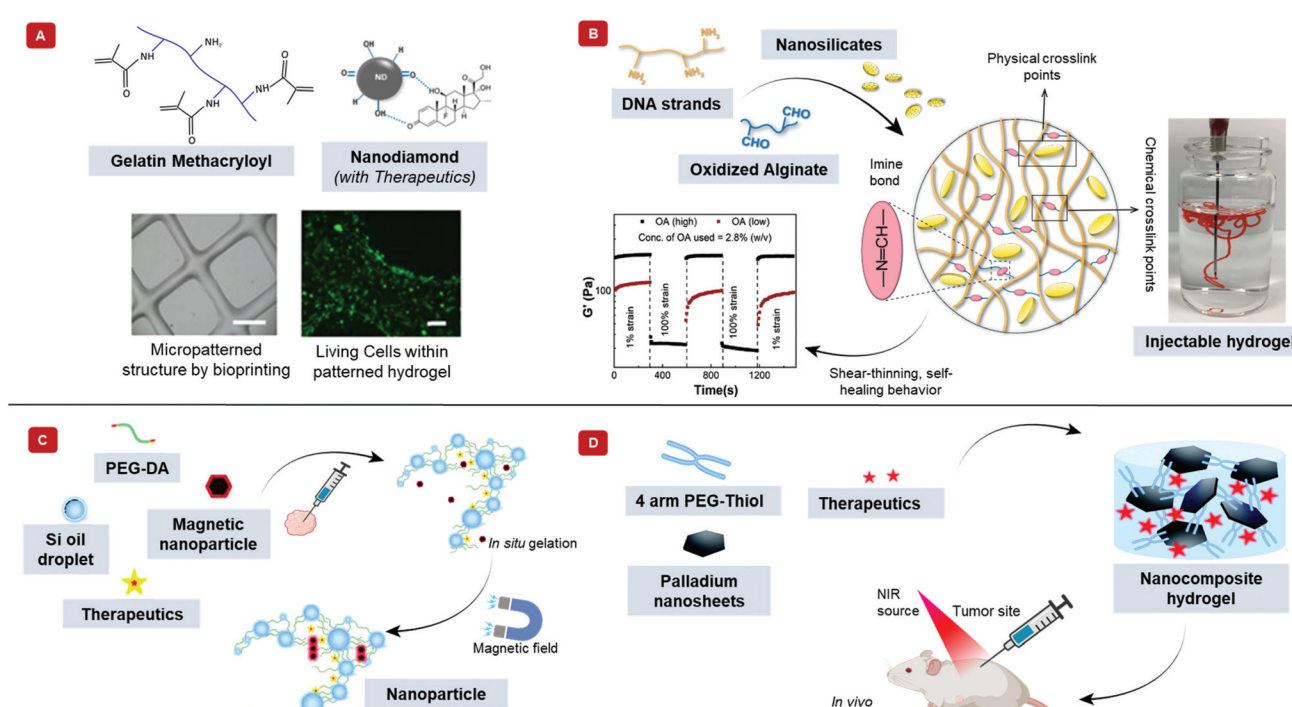


**Fig. 2** Injectable nanocomposite hydrogels for potential bioprinting applications. Injectability is an essential feature of bioinks. The schematic exhibits different nanocomposite hydrogels that are injectable and have the potential to become biomaterial ink. (A) Therapeutics-modified carbon nanodiamonds along with the polymer, gelatin methacryloyl shows injectability. Furthermore, this material can be bioprinted into 3D structures, as shown in the phase contrast image (scale bar = 1 mm). The bioprinted structure can support human adipose-derived stem cells, demonstrated by the green calcein-AM staining after five days of incubation (scale bar = 100  $\mu$ m). Adapted from ref. 42 with permission from Nature Research Group, copyright 2017. (B) Hydrogel made with DNA, oxidized alginate, and nanosilicates show shear-thinning behavior. The aldehyde groups on alginate react with the amine groups in DNA to form chemical crosslinks. The positive charge on nanosilicates interacts with the negatively charged DNA to form physical crosslinks. The image shows the injectability of the nanocomposite hydrogel. The graph displays the self-healing property of the hydrogel, where the hydrogel becomes fluid-like with the application of strain but recovers its shape when the strain is removed. Adapted from ref. 36 with permission Elsevier, copyright 2020. (C) Schematic displays an injectable, nanocomposite hydrogel that can respond to external magnetic fields. Silicone oil in water nanoemulsion of poly(ethylene glycol) diacrylate (PEG-DA), zinc ferrite magnetic nanoparticles, and indocyanine green behave fluid-like at room temperature. However, at body temperature, the acrylates can insert into the oil–water interface, transforming into a solid-like crosslinked hydrogel. An external magnetic field can increase the temperature of the hydrogel by nanoparticle alignment. Adapted from ref. 43 with permission from The Royal Society of Chemistry, copyright 2017. (D) The illustration displays a photosensitive, two-dimensional palladium nanosheet incorporated nanocomposite hydrogel. The hydrogel forms when the nanosheet mixes with 4-arm poly(ethylene glycol)-thiol. Here, palladium reacts dynamically with sulfur of the thiol group to crosslink the polymer. The hydrogel can be loaded with therapeutics, which releases by applying near-infrared light. Adapted from ref. 44 with permission from The Royal Society of Chemistry, copyright 2020.

## 2. Bioink and instrument criteria for bioprinting

Several mechanical, physical, and biological criteria need to be fulfilled by nanocomposite-based hydrogels to qualify as bioinks.<sup>45</sup> Bioinks for extrusion-based 3D bioprinting are generally highly viscous. However, high viscosity compromises cell viability because of increased shear stress on the cells during printing. As a countermeasure, novel strategies in the form of *in situ* photocrosslinking and printing onto a bath are being employed to prepare low viscosity inks.<sup>46–48</sup> Shear-thinning is another important property that allows the bioinks to flow through the printer nozzles. At the same time, high zero-shear viscosity provides stability to the shape of the bioinks. With the help of these properties, bioinks can be extruded in the form of filaments. Once extruded, the filaments can retain their shape until undergoing gelation. Only stable filaments can create complex 3D microstructures. Such structural fidelity requires hydrogel reinforcement.<sup>49</sup> Hydrogel reinforcement can be based on several strategies, including crosslinking mechanism, co-printing with thermoplastics, selected polymeric network, functionalization of the polymers, and incorporating nanoparticles. In this review, we have focused on reinforcing bioinks and biomaterial inks with nanoparticles. Alongside, we have shown how nanoparticles add to the functionality of the polymers involved.

In terms of mechanical properties, the hydrogels can be divided into three main classes: stable hydrogels, self-healing hydrogels, and shear-thinning hydrogels.<sup>18</sup> Stable hydrogels are mechanically sturdy and are usually formed by covalent crosslinking. However, covalent crosslinking may be toxic. Instead, ionic crosslinking, in the presence of nanoparticles, can be another alternative.<sup>50–52</sup> Self-healing hydrogels, on the other hand, have the capability of returning to their original shape upon the removal of the external stimuli that deformed the hydrogel initially.<sup>36,53,54</sup> A host of different mechanisms, including dynamic covalent bonding, hydrogen bonding, ionic bonding, supramolecular interactions, and hydrophobic bonding, can be used to prepare self-healing hydrogels.<sup>55</sup> The shear-thinning category involves mechanically weaker

hydrogels.<sup>35,56,57</sup> The primary mechanism of synthesizing shear-thinning hydrogels involves self-assembly of the different constituent materials.<sup>58</sup> Electrostatic attraction, hydrophobic interaction, and hydrogen bonding favors self-assembly, whereas solvation and electrostatic repulsion works against self-assembly. The weak forces involved here allow for the deformation of the hydrogel under the application of shear forces. Microfiber suspensions have also been shown to have shear-thinning properties, and the alignment of the polymeric network can play a role in the viscosity of such materials.<sup>59</sup> Table 1 highlights some nanocomposite hydrogels based on the crosslinking mechanisms. Other than rheological and mechanical properties that govern the criteria for material selection, the kinetics of gelation, swelling behavior, density, and surface tension of the hydrogel are important physical characteristics to consider for printing.<sup>60</sup> Table 2 lists the salient physical, mechanical, and biological properties of the bioinks.

Among the different properties, rheological ones are extremely critical in defining the characteristics of bioinks and demands further discussion. When considering the printing of nanoparticle-containing bioinks, it is imperative to consider their influence on the printability of the bioink. This section focuses on the effect of nanoparticle additions on the rheological factors of the popular modes of bioprinting.

Any form of syringe-based printing of bioinks roughly translates to extrusion-based bioprinting and gets majorly concerned with whether sufficiently shear-thinning properties are displayed by the bioink to be printed.<sup>61</sup> Another major consideration of extrusion-based bioprinting is the propensity of the shear-thinnable bioink to return to its native viscose state post-passage through the nozzle. This determines the ability to print at a fine resolution. Specifically, two moduli – storage ( $G'$ ) and loss ( $G''$ ) form the chief quantifiable parameters in this regard. Wei *et al.* observed that the addition of bioglass did not negate the excellent rheological characteristics of the alginate-gelatin matrix.<sup>62</sup> The nanoparticle-modified bioink also preserved the duration required for crosslinking the “matrix without the nanoparticles”, thereby having no discernible detrimental effect on the crosslinking mechanism of the hydrogel. In fact, the incorporated bioglass was able to posi-

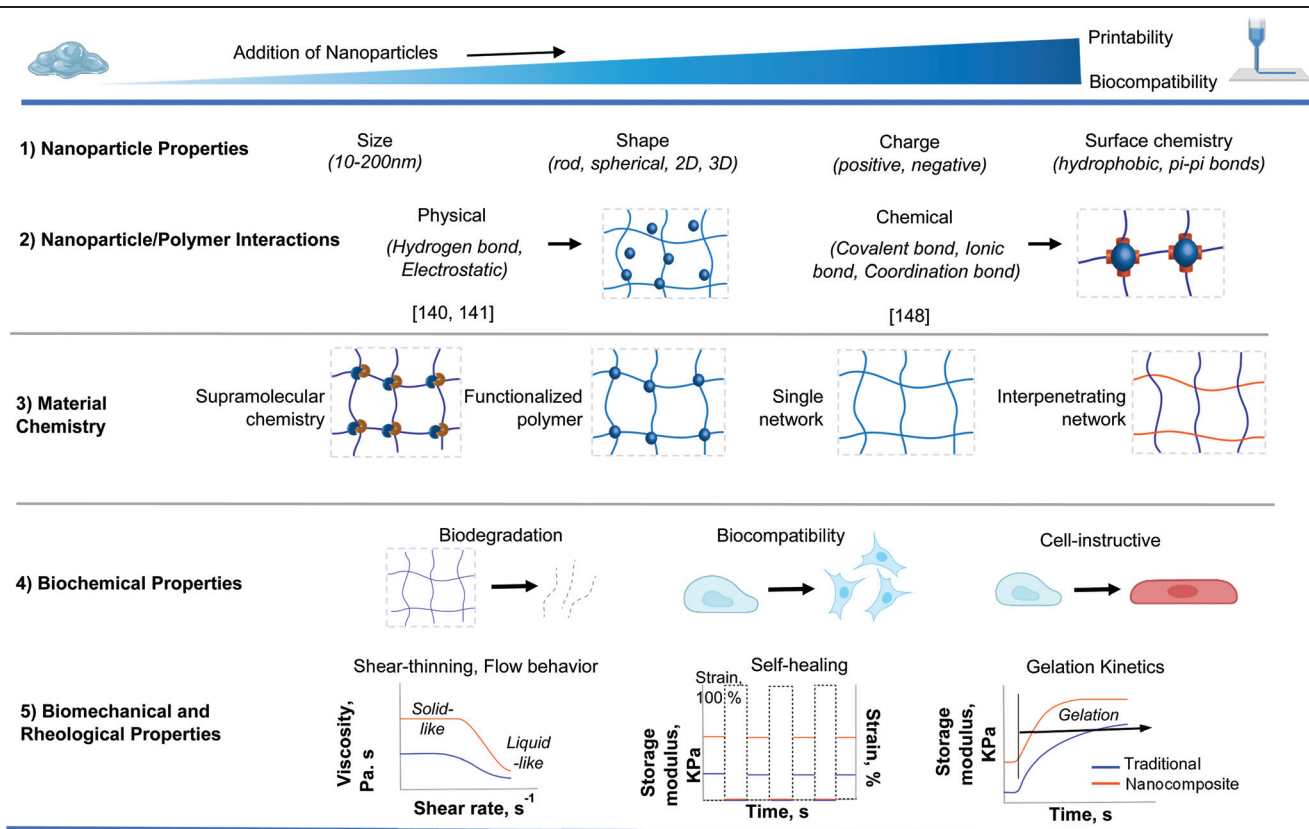
**Table 1** Hydrogel Class

Polymer	Nanomaterial	Crosslinking mechanism	Nanoparticle use/summary	Ref.
Sodium alginate	Graphene oxide	Ionic, physical	Mechanical reinforcement	50
$\kappa$ -Carrageenan/xanthum gum	Halloysite nanotubes/carboxylated-cellulose nanocrystals	Ionic, physical	Mechanical reinforcement	51
Poly(acrylamide-co-acrylic acid)	Cellulose nanofibers	Ionic	Mechanical reinforcement	52
Poly(ethylene glycol)	Cellulose nanocrystals	Covalent, physical	Renewable and reusable hydrogel	36
DNA/sodium alginate	Nanosilicates	Covalent, physical	Hydrophobic drug delivery platform	53
Dialdehyde carboxymethyl cellulose	Cellulose nanofibrils	Covalent	Mechanical reinforcement	54
Polyvinyl alcohol	Nanocellulose	Physical	Improved structural integrity and stability	57
Gelatin	Nanosilicates	Physical	Enhanced physiological stability	56
DNA	Nanosilicates	Physical	Bone regeneration	35

The table outlines the different nanocomposite hydrogels based on the crosslinking mechanism.



Table 2 Material and Instrument properties



The table displays the important properties of bioinks, biomaterial inks, as well as bioprinters. Nanomaterial reinforcement helps improving the printability of traditional hydrogels. However, the material must be biocompatible. Additionally, the table shows significant considerations for the nanoparticle type, nanoparticle/polymer interaction, material chemistry, printing parameters, rheological and biomechanical properties, and biochemical properties.

tively influence the stiffness of the hydrogel matrix by individually increasing their respective diameters and/or by increasing their volume fraction in the bioink. To summarize, an overall improvement in printability was achieved using the bioglass-added bioink, requiring higher pneumatic pressure and a lower nozzle velocity than the bioink containing no nanoparticles.

Laser-assisted bioprinting primarily concerns itself with avoidance of denaturation of the biological materials contained inside the bioink.<sup>63</sup> It should also maintain a high-resolution while printing. Naturally, the addition of nanoparticles into the bioink should add to these complexities. Catros *et al.* demonstrated laser-assisted bioprinting of human osteoprogenitor cells along with a nanohydroxyapatite formulation.<sup>63</sup> The physico-chemical and crystalline characteristics of the nanohydroxyapatite were observed to be slightly modified during printing. This phenomenon occurred, irrespective of the laser pulse energy used, but did not affect the biocompatibility of the bioink. Crucially, ejection of smaller droplets was possible at lower pulse energy. So, micro-scale resolution at lower pulse energy could be achieved using nanoparticles of smaller dimensions (50 nm).

Gao *et al.* used thermal inkjet printing to obtain three-dimensional bone marrow-derived human mesenchymal stem cell-laden scaffolds.<sup>64</sup> The processing involved co-printing with two types of bioactive ceramic nanoparticles – bioglass and hydroxyapatite. The nanoparticles interacted with the live cells during and post-printing. An improvement in the compressive strength of the printed scaffolds was observed in case of the bioglass-embedded locations. Eventually, the bioglass nanoparticle content was shown to have a higher control over the cell viability and rheological characteristic of the bioink.

Addition of nanohydroxyapatite was also noted to improve the compressive strength of an osteochondral scaffolds printed using stereolithography.<sup>65</sup> An improvement in compressive modulus was evidenced in the nanoparticle containing osteochondral scaffold in comparison to the one containing no nanoparticles. Nanotexturization was also evident in case of the nanoparticle modified construct, enhancing the bioactivity of the said scaffolds. An overall idea can therefore be germinated that the incorporation of nanoparticles, in controlled measure, aids the mechanism of bioprinting. This behavior holds true for all the popular modes of bioprinting currently in practice.

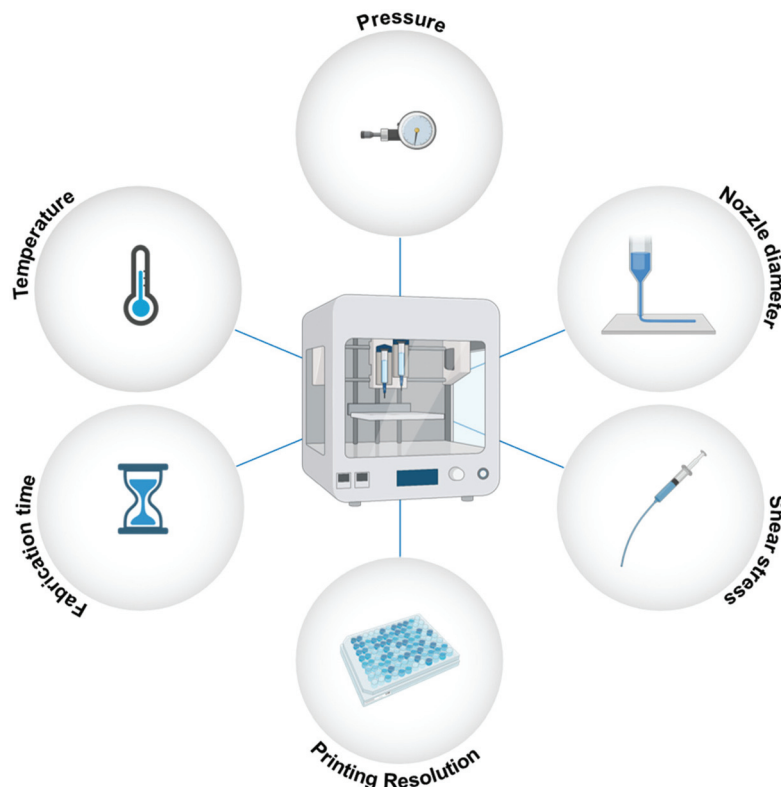


**Fig. 3** Significant printing parameters. The illustration displays the important printing parameters that affect the bioprinted structures. Nozzle pressure and diameter both exert forces on the bioink. Moreover, the shear stress generated on the bioink controls the flow of the filaments. The shear viscosity plays a key role in making the bioink printable as all the forces mentioned above can alter the shear viscosity of the material. Printing temperature is another critical parameter. Since biological materials, including cells, are incorporated within the bioink, high-temperature extrusion processes are not desirable. The fabrication time can control the resolution of the printed structures. High-resolution structures take longer to print.

Other than the discussed material requirements, specific process/instrument parameters define the fate of the bioprinted microstructures.<sup>66,67</sup> Fig. 3 illustrates the essential process parameters that should be considered for bioprinting. Shear stress is a vital instrument parameter when the bioink is being extruded from nozzles. The applied shear stress is dependent on several factors, such as the extrusion pressure, the diameter of the nozzle, the print speed, and the viscosity of the material being printed.<sup>68</sup> Shear stress can have a severe effect on cellular processes and may alter cell signaling and protein expression. Bioinks with high viscosity and small nozzle diameters are favorable for high-resolution bioprinting. However, both these conditions can lead to excessive shear stress on the cells, and to avoid any adverse effects, a delicate balance needs to be struck between the applied shear stress and the bioprinting resolution. The applied temperature is another important process parameter to consider for bioprinting. Both cell viability and material viscosity are dependent on the temperature at which the bioprinting is carried out. Excessive temperatures are not suitable for living cells, and therefore, high-temperature methods like thermal inkjet printing are not feasible for tissue engineering-based applications.<sup>69</sup> Another important instrument parameter is the fabrication time of the 3D microstructure. Higher resolution

prints are time-consuming. Enhanced motor control, nozzles, or syringes may be able to reduce the fabrication time for high-resolution bioprinting.<sup>1</sup> Therefore, both material properties and instrument parameters must be carefully examined for bioprinting.

### 3. Nanoparticle induced functionalities

#### 3.1. Mechanical functionality

Hydrogels made from purely natural polymeric sources and lacking any reinforcement strategy fail under mechanically demanding conditions.<sup>70</sup> Such conditions are abundantly found in the load-bearing bone and cartilage tissues.<sup>71</sup> Although increasing polymer concentration and crosslinking density solve this problem to an extent, they have a negative impact on the rates of nutrient content, bioactive factor, and cell metabolite flux through the hydrogel. The mechanical properties of hydrogel scaffolds must also be perfectly congruent with those of the surrounding tissues during *in vivo* conditions. Nanocomposite hydrogels have been shown to exhibit extremely high levels of resistance to deformation in terms of twisting, knotting, tearing, and bending. Therefore, the incor-

poration of nanoparticles is a suitable strategy for enhancing mechanical behavior.

For nanocomposite hydrogels and biomaterial inks, the usual mechanically reinforcing nanoparticles include nanoclay,<sup>72</sup> graphene nanosheets,<sup>73</sup> carbon nanotubular structures,<sup>74</sup> and polymeric nanoparticles,<sup>75</sup> mesoporous silica<sup>76</sup> among others,<sup>62,77</sup> that enhance their printability as well. Nanoclays (popularly referred to as nanosilicates) have been extensively applied as mechanical reinforcements for hydrogels and biomaterial inks.<sup>36,78</sup> Fig. 4A displays a nanosilicate reinforced bioink. Usually dimensioned at 1 nm thickness and diameters in the range of 25–100 nm, they have permanently charged surfaces, with negative charges residing on either face and positive ones on the circumference (if imagined like a 2D disc). This morphology, (and the extraordinarily high surface charge density associated thereof) is what makes them highly suited to form strong electrostatic linkages with the polymeric chains of the bioinks they are meant to reinforce. The reversible nature of these linkages, along with those existing among the nanosilicates themselves help distribute the load experienced under duress.<sup>49</sup> All these functionalities of nanosilicates

proved them to be conducive for bone tissue engineering applications as well. However, nanosilicates may also be added to bioinks to sustain the release of therapeutics. Fig. 4B shows a nanosilicate incorporated biomaterial ink that releases growth factors.<sup>79</sup>

Adding nanoparticles to enhance the mechanical properties of thermally responsive injectable hydrogels to render them printable is also in practice.<sup>80</sup> This is somewhat different from the usual enhancement in mechanical properties using nanoparticles. Here, the added nanoparticles must improve upon, or at least maintain the same level of thermo-responsiveness, as was associated with the native hydrogel base. Poly(*N*-isopropylacrylamide) – pNIPAM hydrogels – a popular class of negative thermosensitive polymers, can be rendered printable with the addition of silicon-based nanoparticles.<sup>81</sup> Zhang *et al.* achieved a 5-times heightened thermo-responsive activity of a native pNIPAM based hydrogel by the addition of single-walled carbon nanotubes.<sup>82</sup> A vital advantage of thermo-responsive nanocomposite materials is their ability to be printed into scaffolds of intricate geometry through the recently evolved 3D printing-guided thermally induced phase separation tech-

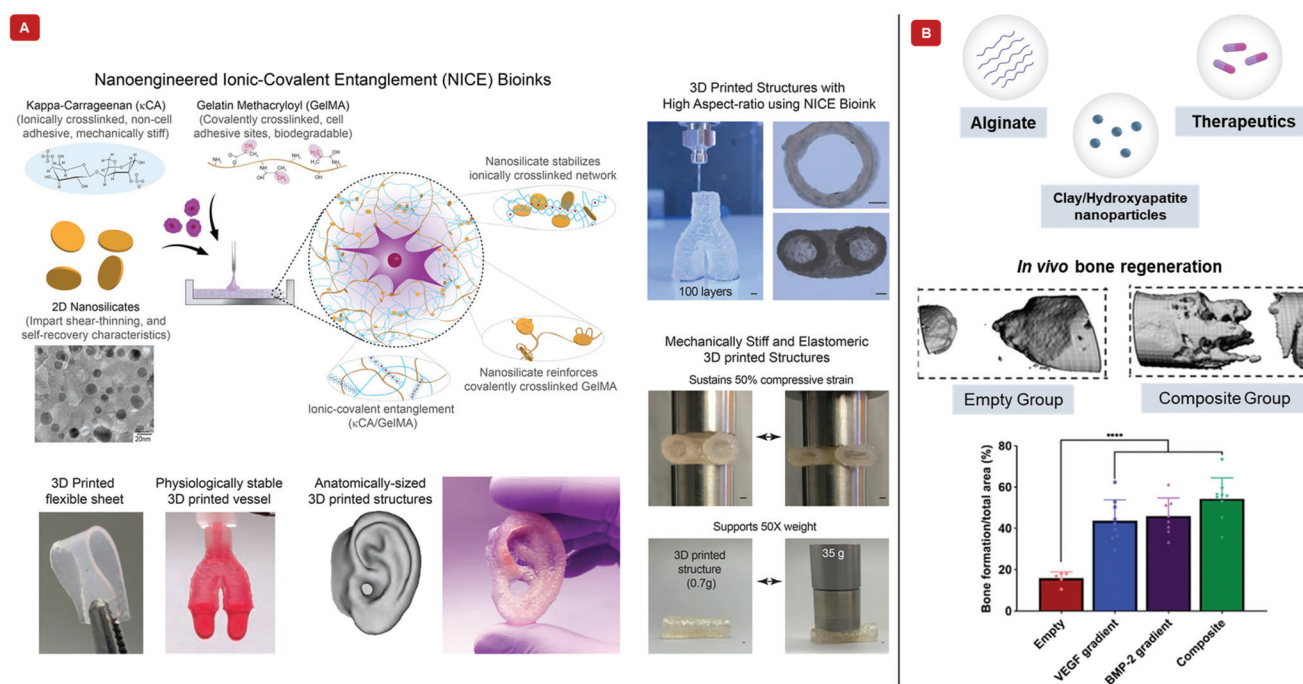


**Fig. 4** Bioprinting with nanocomposite hydrogel-based bioinks and biomaterial inks. (A) The illustration demonstrates a nanoengineered ionic-covalent entanglement, "NICE", bioink interpenetrated with ionically crosslinked  $\kappa$ -carrageenan and covalently crosslinked gelatin methacryloyl. The bioink is mechanically reinforced with nanosilicates. The transmission electron micrograph shows a uniform dispersion of the nanosilicates. The NICE bioink fabricated 3D structures have high structural fidelity, as shown in the images (scale bar = 1 mm). Complex structures can be printed with this bioink. Furthermore, the 3D structures can sustain compressive forces and support 50 times their weight. Adapted from ref. 40 with permission from The American Chemical Society, copyright 2018. (B) Schematic displays the components of a growth factor releasing biomaterial ink. The polymer background is made of covalently crosslinked methylcellulose and sodium alginate. Nanoclay or hydroxyapatite nanoparticles have been used to control the release of therapeutics in the form of growth factors. The growth factors have been delivered as a gradient with maximum concentration at the center to no growth factor at the boundary. *In vivo* MicroCT images capture the healing of bones after 12 weeks from surgery. Area analysis from histological stains shows enhanced bone formation when two growth factors, vascular endothelial growth factor (VEGF) and bone morphogenetic protein 2 (BMP-2), have been simultaneously delivered with the bioinks. Adapted from ref. 79 with permission from The American Association for the Advancement of Science, copyright 2020.

nique. As has been evidenced by Wu *et al.* this method has been successfully used to create a poly(urea-urethane) based thermo-responsive nanoscaffold.<sup>83</sup> They controlled the mechanical properties of the scaffolds through regulation of the phase separation temperature which had a direct effect on the porosity and phase structure keeping the external architecture of the construct, constant.<sup>83</sup>

Nano-hydroxyapatite<sup>84</sup> and nanoclay<sup>80</sup> incorporated block copolymers showed thermoresponsiveness similar to that of the native polymers, with the nanoparticles lending the much-needed mechanical attributes appropriate for injectability. A similar effect on pure kappa-carrageenan ( $\kappa$ CA), a biopolymer developed from red algae, was established through the work of Wilson *et al.* where nanosilicate compositions significantly lowered gelation temperatures and exhibited high shape retention after the printing.<sup>85</sup> Nanomaterial optimized mechanical strength is, therefore, a vital property for biomaterials to be printed for applications in tissue regeneration, wound healing, drug delivery, and so on.

### 3.2. pH-Responsive functionality

pH responsiveness is of paramount importance considering biomedical applications.<sup>86–89</sup> Silica nanoparticles have been suitably employed in this regard to fabricate a class of injectable hydrogels having supersensitivity to pH changes.<sup>90</sup> While this hydrogel remained relatively stable in neutral environs, it underwent rapid gelation in even weakly acidic conditions, altering its mechanical, rheological, and degradation characteristics. This remarkably pH-sensitive gelation has been attributed to Schiff base reactions occurring between the amine groups of the functionalized silica nanoparticles and the aldehyde functionalities of the polymeric components. The resultant imines formed from the Schiff base reactions were also responsible for the dynamically reversible cross-linking mechanism necessary for rendering shear thinning properties.

Swelling behavior is treated as a significant marker in determining the effect of pH, which also formed the crux of delivering drugs and other microconstituents. This parameter has usually been found to be dependent on the surface functional group, which causes hydration or shrinkage at different pH levels. A low addition of carboxylated and hydroxylated nanodiamond to hyaluronic acid enabled the resulting nanocomposite hydrogel to possess a higher compressive force and gel breakage point at strain values higher than those of the unmodified parent hydrogel itself upon being printed.<sup>91</sup> The functionalized nanodiamond clumped structures after being dispersed had pH-dependent diameters. The rheological properties of these hybrid gels were assessed in terms of their storage and loss moduli, both of which were found to be more enhanced in the presence of basic media. Consideration of these properties were vital in the light of printability, gelation being dependent on these two moduli values. These studies show the possibility of formulating nanocomposite hydrogel-based bioinks with pH-responsive functionalities.

### 3.3. Electroconductive functionality

Nanomaterials have been extensively chosen to induce electroconductivity to develop biosensors, target-specific drug delivery vehicles, and even bioelectrodes for *in vivo* implantation. They are also deemed highly appropriate for application as electroactive substrates or scaffolds in tissue engineering or even as drug delivery agents, releasing their load in response to electrical stimuli. Such nanocomposite materials have the added advantage of printability through shear-thinning characteristics being simultaneously improved by their incorporation. Traditionally, carbon nanotube,<sup>92–94</sup> graphene,<sup>95</sup> and gold-based nanoparticles<sup>96,97</sup> have been used in hydrogels for bioprinting conductive structures.<sup>98,99</sup> Multiple studies in the recent past have established nanotubes as one of the most suitable candidates for hydrogel-based scaffolds meant to be extensively applied in cardiac tissue engineering.<sup>100,101</sup> This choice has been substantiated by the significant improvements in cell–cell coupling and superior facilitation of signal propagation brought about by these carbon-based nanoparticles.<sup>102</sup> Shin *et al.* have successfully carried out the development of carbon nanotube-based biomaterial inks.<sup>103</sup> These biomaterial inks were effectively stabilized using DNA, hyaluronic acid along with gelatin. The authors had efficiently embedded printed circuitry within hydrogels paving the way for developing biosensors or foldable functionalized scaffolds for tissue engineering. However, the application of nanotubes has often been plagued by cytotoxicity concerns considering their clinical practice as well as low solubility issues.<sup>104,105</sup> Although effective modification technologies through coating and functionalization<sup>106</sup> have evolved, causing a significant decline in their cytotoxicity levels, they have also been responsible for diminished electroconductivity. Therefore, the biomedical applications of such carbon-based nanostructures remain to be explored in the context of optimizing electroconductive hydrogels through simple fabrication routes and with permissible cytotoxicity limits.

Among the metallic nanoparticles, gold incorporated polymeric scaffolds have been found to be potential candidates for imparting electroconductive behavior. Zhu *et al.* have been successful in developing a gold nanorod infused gelatin methacryloyl (GelMA) based bioink to regenerate and support cardiac tissue, effectively coupling adjacent cardiac tissues through its electroconductivity.<sup>96</sup> Therefore, a plethora of nanomaterials can be loaded inside hydrogels to create printable electroconductive formulations for suitable applications in tissue engineering. However, further research must be conducted to assess the biocompatibility of these nanomaterials while maintaining their electroconductive characteristics.

### 3.4. Photo-responsive functionality

Near-infrared absorbing nanoparticles have light to heat energy conversion capabilities. The swelling and mechanical properties of hydrogels with such nanoparticles can be desirably modified by altering their exposure to light, going on to produce perceptible changes in the temperature of their



immediate environments.<sup>107</sup> The resulting local rise in temperature can have an antimicrobial effect, ensuring a direct application in wound dressings.<sup>108</sup> The nanomaterials capable of responding to such changes in luminous intensities popularly include gold nanorods,<sup>109</sup> polymeric nanoparticles,<sup>110</sup> among others.<sup>111,112</sup> Recent applications have focused on facilitating the delivery systems of such nanocomposite hydrogels, improving their injectability in the process. Yang *et al.* demonstrated this line of development by designing a nanocomposite hydrogel with tungsten disulfide nanosheets, lending photothermal-responsiveness through their high efficiency of heat-to-light energy conversion.<sup>113,114</sup> Shear-thinning at high shear rates and a corresponding reversible thixotropic behavior confirmed the injectable nature of this formulation. An additional finding of this study was the light-mediated release of antibiotic drugs on-site. The combined effects of photothermal as well as drug induced healing therapies were thus observed to sufficiently bolster the process of wound healing.

Gold-based nanoparticles have been extensively used for similar photothermal therapeutic measures, although they have been plagued by their tendency to seep across vascular barriers and consequently having lower efficiency of photosensitivity. Through suitable modification of these nanoparticles, as has been carried out by Zeng *et al.*, gold nanoparticles have been retained at their proper sites.<sup>115</sup> This has been possible through mussel-inspired adhesive strategies, brought about by coating them, to influence their interaction with the hydrogel network. The injectability of this strategic nanocomposite hydrogel was evident from the temperature-dependent gelation times. The essential attributes of photothermal therapy and injectability characterizing photo-responsive nanocomposite hydrogels, therefore, promise an explosion onto the biomedical research scene soon, to be tested for application in drug delivery, wound healing, and other therapeutic applications, including cancer therapy.

### 3.5. Magnetic field-responsive functionality

Magnetic nanocomposite hydrogels have been extensively experimented upon.<sup>116–118</sup> Usually, the nanoparticles employed include iron (Fe), cobalt (Co), nickel (Ni), or oxides like  $\gamma$ -Fe<sub>2</sub>O<sub>3</sub>, Fe<sub>3</sub>O<sub>4</sub>, and CoFe<sub>2</sub>O<sub>4</sub>. With the help of external magnetic field-based stimuli, these nanoparticles can be aligned, causing a locally induced hyperthermia through Néel and Brownian relaxations,<sup>119</sup> which effectively heats the adjacent hydrogel matrix.<sup>120</sup> These externally controllable local rises in temperature bring about alterations in the shape and volume of the hydrogel matrix.<sup>121,122</sup> Tseng *et al.* established a simplistic assaying technique using magnetic nanoparticles, gold, iron oxide, and poly-L-lysine, embedded cells printed into spheroids by magnetic 3D bioprinting.<sup>123</sup> The need for having a 3D cellular model was necessary to factor in the effects of cell-cell and cell-extracellular matrix interactions, lacking in 2D systems. These spheroids displayed toxicity-specific rates of contraction, allowing for the high-throughput detection of the level of toxicity. The presence of the embedded magnetic nanoparticles allowed the cells to be easily printed through directed mild

magnetic forces. Kim *et al.* used a cobalt ferrite nanoparticle incorporated poly (organophosphazene) hydrogel where hydrophobic interactions were primarily responsible to bind the surface of the nanoparticles to the L-isoleucine ethyl esters groups prevalent on the polymer chains.<sup>121</sup> The resulting hydrogel displayed excellent thermosensitivity through reversible sol-gel phase transition. Injectability was an important attribute of this concoction, as the gel was injected into a rat brain, enabling long-term magnetic resonance imaging. Such hydrogels helped detect diseased tissue by inducing local spikes in temperature and magnetic resonance imaging, allowing their treatment through inductive heating and remote-controlled drug release. An emerging application of magnetic nanoparticles in 3D bioprinting involves the use of Gadolinium (Gd<sup>3+</sup>) chelates as paramagnetic agents to assemble tissue spheroids through magnetic levitational bioassembly in space (microgravity conditions).<sup>124</sup> Moreover, magnetic hydrogels have also been shown to have great potential in developing sensors, nanomotors, robot-like soft actuators, and a motley of separation devices.<sup>124,125</sup>

### 3.6. Miscellaneous functionalities

The underlying characteristic of the nanocomposite hydrogels of our interest is their injectability or printability. Although nanoparticles are responsible for inducing various functionalities, and sometimes even more than one simultaneously, only a handful of them satisfy this criterion. In a way, all the nanocomposite hydrogels discussed so far are multifunctional in essence, for they have the basic injectability property in addition with another specialized functionality. However, we shall now turn to such nanocomposites, which offer more than two functionalities. These multi stimuli-sensitive hydrogels are developed through a strategic concoction of select nanoparticles. Hooshyar and Bardajee demonstrated the applicability of a dual thermo- and pH-responsive silver-based nanocomposite as drug delivery vehicles.<sup>126</sup> Similarly, pH-mediated characteristic of hydrogel nanocomposites has been reported indirectly, due to the presence of gold nanoparticles along with modified doxorubicin – a drug, in an injectable polymeric hydrogel. The modifications in doxorubicin were primarily behind the pH-sensitiveness of this formulation, while the gold nanoparticles, being near-infrared responsive, stimulated the release of the drug through rupture of the hydrogel networks. Correspondingly, a remotely controllable steady release of the drug was mediated using nanoparticles.<sup>127</sup>

Upconverting nanoparticles are a class of nanoparticles that can absorb two or more photons in the infrared range of the spectrum and emit a single photon of significantly higher energy, belonging to the UV region of the electromagnetic spectrum. Strontium fluoride, SrF<sub>2</sub> upconverting nanoparticle-based, lanthanide ion-doped core-shell nanocomposite hydrogels were successfully fabricated using magneto-responsive iron oxide nanoparticles.<sup>128</sup> The magnetic self-assembly allowed for remotely controlled variations in the structure of the printed hydrogel. Fig. 5 shows a digital light processing

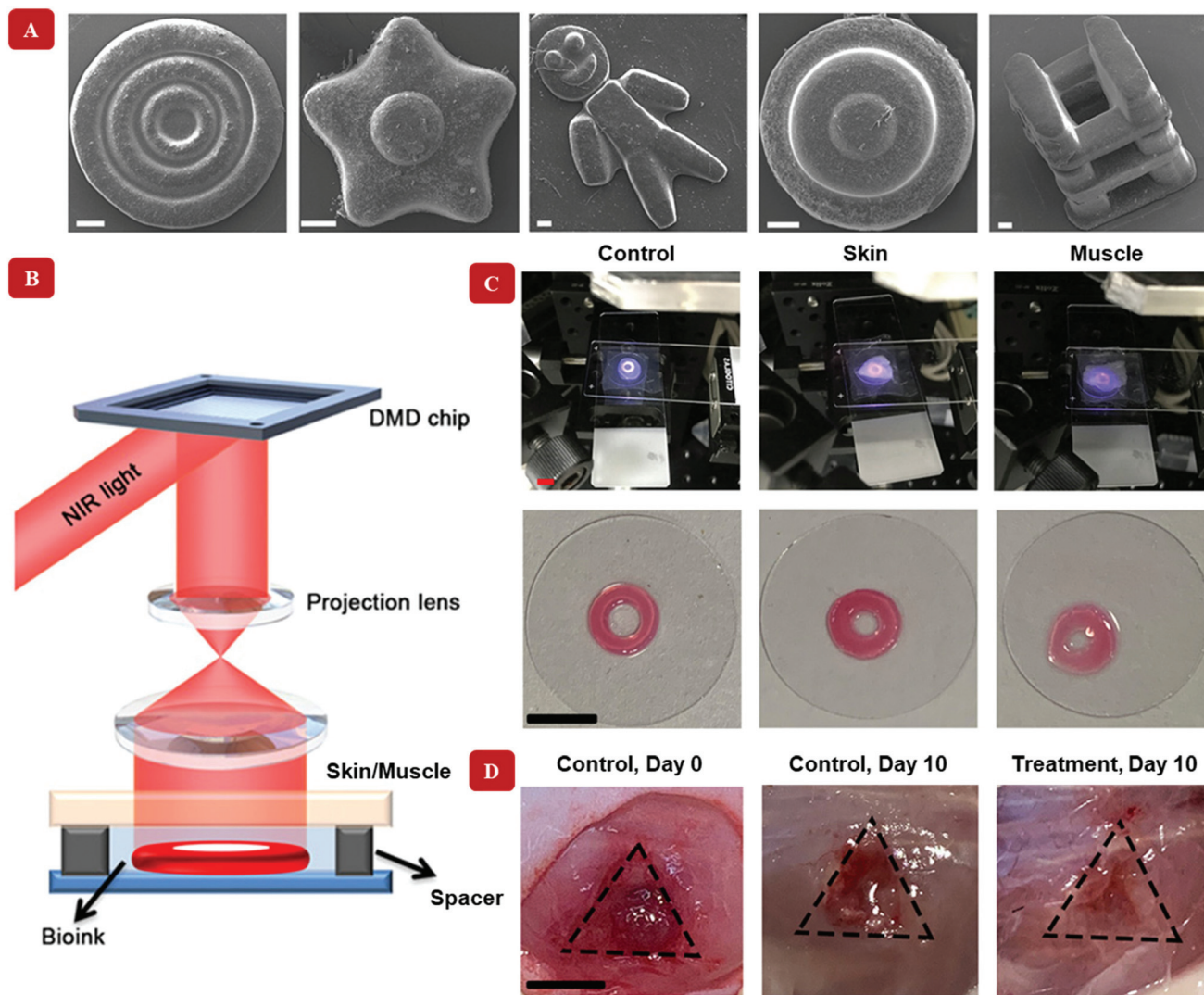


**Fig. 5** Digital Light Processing bioprinting with nanocomposite hydrogel-based bioinks. Unlike extrusion-based methods, a light-assisted bioprinting technique has been shown in this figure. Upconverting nanoparticles coated with the photoinitiator lithium phenyl-2,4,6-trimethylbenzoylphosphinate have been used to crosslink the polymer gelatin methacryloyl. (A) Multiple shapes have been printed with the bioink (scale bar = 200  $\mu\text{m}$ ). (B) Illustration reveals the *in vitro* bioprinter setup. Here, near-infrared light at 980 nm is passed through a digital micromirror device (DMD), which timely projects the light onto a lens. The timely projected, patterned light can penetrate through skin/muscle barrier. The upconverting nanoparticle coated with the photoinitiator converts the light to 365 nm at which gelatin methacryloyl undergoes gelation and produce desired shapes. The bioink without any barrier has been designated as a control in this case. (C) The bioink is injected into the subject, where gelation occurs by shining near-infrared light. Therefore, this is a non-invasive method of healing wounds. The images display the healing process after 10 days from the treatment. Adapted from ref. 129 with permission from The American Association for the Advancement of Science, copyright 2020.

bioprinting technique that involves upconverting nanoparticles.<sup>129</sup> Multi-material nanocomposite hydrogels have also been hybridized to stitch together specific functionalities like anti-microbial,<sup>130</sup> electroconductive,<sup>131</sup> magneto-sensitive,<sup>132</sup> and so on.<sup>113</sup> Table 3 summarizes the different functionalities that are imparted by nanomaterials. These properties can be exploited to prepare advanced nanocomposite hydrogel-based materials suitable for bioprinting. Beyond the category of external stimuli-responsive functionalities, the following section discusses the biological features of the designed bioinks that can make them suitable for clinical translation.

#### 4. Biocompatibility and biofunctionality of nanocomposite bioinks

The biocompatibility of any material can be defined as its ability to support cell viability. Cell viability assays are routinely reported in the literature to evaluate cell-material interactions.<sup>133,134</sup> These assays are especially important when nanocomposite materials are used because of their probable cytotoxic effects. Several parameters must be thoroughly studied, including size, shape, structure, surface charge, and

**Table 3** Functionalities imparted by nanoparticle-hydrogel composite

Functionality	Nanoparticle	Nanoparticle modification	Polymeric base	Nanoparticle polymer interaction	Applications	Additional references
Mechanical property <sup>73</sup>	Graphene Oxide sheets	—	Alginate + CaCl <sub>2</sub>	Hydrogen bonds between functional groups attached to nanoparticle surface and hydroxyl groups on calcium alginate	Improving printability	40, 78 and 84
pH responsive <sup>91</sup>	Nanodiamonds	Surface functionalized to possess carboxyl and hydroxyl groups	Hyaluronic acid	Hydrogen bonds based on pH level	Soft yet robust printable nanocomposite materials	87–89
Electro-conductive <sup>103</sup>	Carbon nanotubes	DNA-coated	DNA and hyaluronic acid	$\pi$ - $\pi$ stacking interactions between carbon nanotubes and DNA bases, along with hydrogen bonding and hydrophobic interactions	3D flexible electronics	74, 93 and 94
Photo-responsive <sup>184</sup>	Tungsten disulfide nanosheets	Decorated with L-cysteine and loaded with ciprofloxacin drug	Dodecyl-modified chitosan stabilized by dialdehyde-functionalized poly-ethylene glycol	Colloidal dispersion of the modified nanoparticles occurs	Photo-thermal drug delivery	111, 112 and 127
Magnetic field responsive <sup>121</sup>	Cobalt ferrite (CoFe <sub>2</sub> O <sub>4</sub> )	—	Poly-organophosphazene	Hydrophobic interactions	Long term magnetic resonance contrast platform system	117, 118 and 120

The table highlights the different external-stimuli responsive properties of primarily injectable nanocomposite hydrogels that may have potential bioprinting applications in the near future.

concentration of the nanoparticles when evaluating their potential for diverse bioprinting and regeneration therapy applications.<sup>135</sup> These parameters are dependent on the material under consideration. As an example, silver nanoparticles show greater cytotoxicity when small particles (generally within 20 nm) are used.<sup>136</sup> The reason for this adverse behavior can be ascribed to the generation of cytotoxic reactive oxygen species, which depends on the size of the nanoparticles in use. Smaller-sized nanoparticles tend to generate higher amounts of reactive oxygen species and have a greater detrimental impact on cells. The shape of the nanoparticles may also contribute to an increase in the production of reactive oxygen species.<sup>137</sup> Another major concern with biocompatibility arises from the possibility of nanoparticles triggering undesired immune responses.<sup>138</sup> The presence of hydrophobic components on the nanoparticle surface usually leads to unwanted triggering and subsequent inflammation. Chemically modifying the surface of the nanoparticles can significantly improve the biocompatibility of the nanoparticles. For example, Qu *et al.* coordinated titanium sulfonate ligand to black phosphorous nanosheets to enhance the biocompatibility of the nanomaterial.<sup>139</sup> The titanium-based ligand reduced the degree of oxidation of black phosphorous, thereby decreasing the generation of reactive oxygen species. Similar surface chemical modifications can increase the biocompatibility of nanoparticles. Only biocompatible, cell-supportive nanoparticles should be considered when designing nanocomposite hydro-

gel-based bioinks for successful clinical translation. However, the interaction between nanoparticles and polymers can alter the cell-instructive behavior of both the nanoparticles and the polymers. Therefore, the biocompatibility and biofunctionality of the polymers combined with the nanoparticles must be carefully evaluated before preparing bioinks. At present, cell viability assays, such as calcein acetoxymethyl (calcein AM) staining and tetrazolium reduction-based assays, are commonly used to determine the biocompatibility of different nanocomposite materials for 3D bioprinting applications.<sup>140–142</sup> Additionally, special attention must be given to ascertain that such nanocomposite materials do not induce any significant phenotypic and global gene expression profile changes within the exposed cells.<sup>67,143</sup> It is imperative to carry out a routine examination of cell surface markers to confirm the stability of the cellular phenotypes once exposed to the various nanocomposites.<sup>144</sup> Outside the field of bioprinting, studies involving phenotypical analysis of cells are frequently tested for nanotoxicological assessment.<sup>145</sup>

On the other hand, biofunctionality means the ability of the nanocomposite hydrogel bioink to (i) aid in cell growth and cell proliferation, (ii) provide mechanical support to the cells, and (iii) impart biological cellular functionalities. Among different nanomaterials, bioactive inorganic nanofillers have been successfully used to incorporate additional functionalities and properties to the bioprinted tissue structures, including enhancing various biological and mechanical



Table 4 Cell-laden nanocomposite bioinks

Hydrogel matrices (composition w/v%)	Nanomaterials (composition w/v%)	Living cells	Tissue engineering application	Ref.
Gelatin (1–4%) /alginate (3–10%)	Bioactive glass (2–7) %	Mouse bone mesenchymal stem cells	Bone	77
Gelatin/alginate (10/1)%	Bioglass nanoparticles (0.5–2) %	Mouse dermal fibroblasts	Multiple	62
Alginate (8%) – hyaluronic acid (5%)	Manganese silicate nanospheres (0–2%)	Murine-derived macrophage cell line RAW 264.7 & Murine umbilical vein endothelial cells	Vascular	153
Alginate (2–3) w/v%	Alpha-tri calcium phosphate (2–6) w/w%	Mouse osteoblasts	Multiple	26
Collagen (5%)	Gold nanowires (0.05%)	Mouse myoblasts (C2C12)	Muscle	97
Hyaluronic acid (5%)/alginate (1%)	Ti <sub>3</sub> C <sub>2</sub> MXene nanosheets (1%)	Human embryonic kidney 293	Multiple, neural	140
Chitosan (2%), alginate (3%)	Nano-bone like hydroxyapatite (0.2%)	Mouse MC3T3-E1 pre-osteoblast	Bone	12
Gelatin methacrylate (10%) + polyethylene glycol diacrylate (5–20) %	TGF-β1-embedded core-shell nanospheres (1%)	Human bone marrow mesenchymal stem cells	Cartilage	9
Alginate (2%) – methylcellulose (2–4) %	Nano hydroxyapatite (2.5 × 10 <sup>-5</sup> %)	Porcine marrow mesenchymal stem cells	Multiple	10
Methacrylated-collagen (0.6%), alginate (2.5%)	Carbon nanotubes (1%)	Human coronary artery endothelial cells	Cardiac	74
Agarose (0.3–1.0%)/collagen (0.1–0.3%)	Streptavidin-coated iron nanoparticles (10 v/v%)	Human knee articular chondrocytes	Cartilage	117
Platlet-lysate (18%)/alginate (4%)/hyaluronic acid (0.4%)	Cellulose nanocrystals (1.22–2.88) %	Human adipose tissue derived stem cells	Multiple	13
Alginate/methyl cellulose (3/9) w/v%	Nano-silicate clay (3 w/v%)	Human mesenchymal stem cells	Skeletal	72

The table highlights nanocomposite hydrogel-based bioinks that are being applied in different tissue engineering applications.

strengths.<sup>146,147</sup> These potential bioactive nanofillers, such as calcium phosphate/hydroxyapatite,<sup>148</sup> silica,<sup>149</sup> bioactive glass,<sup>150</sup> and nanoclay/LAPONITE®<sup>151</sup> can promote bone mineralization and can also release growth factors and other therapeutics locally to further improve the biofunctionality of the tissue construct. Mesoporous silica nanoparticles have also been used for similar purposes.<sup>152,153</sup> Here, mesoporous silica nanoparticles could control the release of growth factor, bone morphogenic protein-4, to promote bone repair. Table 4 shows some recently developed bioinks that contain nanoparticles in the mixture. With tunable biofunctionalities and cell-instructive properties, the next generation of bioprinted tissue structures using combinations of biocompatible materials and nanoparticles look promising.

## 5. Discussion and future outlook

3D bioprinting is a precise technique for fabricating tissues and organs both *in vitro* and *in vivo*.<sup>154–157</sup> Hydrogels are commonly used as bioinks because of their favorable biological properties, allowing the printed cells to adhere, proliferate, and differentiate into desired lineages.<sup>158</sup> Although hydrogels are excellent mimics of the native cellular microenvironment, purely polymeric hydrogels need some form of reinforcement to enhance their mechanical and structural integrity. As illustrated in this review article, hydrogels can be reinforced with various types and forms of nanoparticles to increase their mechanical energy dissipation capabilities and fracture energy

with nominal changes in hydrogel polymeric composition. In addition to providing mechanical stability, these nanoparticles can impart distinctive, external stimuli-responsive material properties to the purely polymeric hydrogels.<sup>159</sup> Material properties, such as photo-responsiveness, pH-responsiveness, and so on, can add to the overall applicability of the 3D bioprinted structure.

Although very promising, nanocomposite hydrogel-based bioprinting applications have certain limitations that have to be overcome. For instance, the potential cytotoxicity of the nanoparticles must be carefully assessed before they can be applied in the medicinal field. The complexity in understanding nanoparticle-tissue interactions has resulted in a paucity of studies where biocompatibility, biodegradability, and eventual fate of nanoparticles in host system have been evaluated in a systematic manner. Characterizing how the shape, size, composition, and physicochemical properties of the nanomaterials affect the immune system is also another area that needs thorough investigation. Nonetheless, the few research studies on this topic demonstrate that if the nanoparticles are not biodegraded and eliminated by the host, it may lead to biochemical toxicity over time. Hence, strategies that require lesser concentrations of nanoparticles may be looked upon as a preferred approach.<sup>160</sup> Biodegradation of the printed microstructures is another concern, especially in the case of grafting-based applications. One solution may be incorporating nanoparticles that increase in temperature in the presence of near infrared light. As for example, near infrared light can heat nanosheets of transition metal dichalcogenides, like tungsten



disulfide.<sup>161</sup> Such nanoparticles may allow users to thermally-degrade the bioprinted microstructures actively. Additionally, these two-dimensional nanoparticles have sulfur-vacancy sites that can be used to bind to thiolated ligands.<sup>162</sup> This property has been exploited to form cell-encapsulating hydrogels, and this material can be implemented in bioprinting applications.<sup>163</sup> Other than material-based disadvantages, there seems to be a lack of approval from federal agencies regarding nanocomposite hydrogel-based bioinks. The approval from federal agencies would be a critical requirement for the clinical viability of these bioinks. Overcoming these limitations will increase the use of such bioinks and will open doors to other unique applications.

Intraoperative bioprinting is another exciting area in health-care technologies where nanocomposite bioinks can be used. Here, 3D microstructures are directly printed on live subjects at the location of injury. Certain material requirements need to be fulfilled for such *in vivo* applications. (a) The material must be clinically approved and inexpensive. (b) The material must be compatible with the mode of bioprinting suitable for quick surgical procedures. (c) The material must also be able to rapidly crosslink and retain shape-fidelity. The addition of nanoparticles can enhance the properties of bioinks and make them suitable for intraoperative bioprinting. For example, glycosaminoglycan nanoparticles along with LAPONITE® can form rapidly crosslinkable bioinks.<sup>164</sup> At present, *in situ* skin grafting is the most common form of intraoperative application.<sup>165,166</sup> However, the ultimate aim is to bioprint entire organs *in situ*. Therefore, more materials need to be explored for advancing this field. Incorporation of nanoparticles into the traditional bioinks can offer multiple advantages to add to the cause and push intraoperative bioprinting technology from bench to clinical bedside and reduce patient hospitalization time. However, regulatory issues at both institutional and government stages must be addressed prior to translation of such bioprinting technologies into clinical practice. Specifically, regulatory approval of bioprinted scaffolds for successful clinical translation can be pretty intricate since they can be considered concomitantly under biologics, drugs, or medical device categories.

Designing bioprints that can mimic the complex, anisotropic structure of the articular cartilage is another possible direction where nanocomposite hydrogel-based bioinks can be effectively used. The articular cartilage consists of dense extracellular matrix with dispersed specialized cells, called chondrocyte.<sup>167</sup> Moreover, they have four zones, superficial, middle, deep, and calcified. These four zones have different biological and mechanical properties, and artificially mimicking this complexity is challenging. Recently, growth factor releasing bioinks were designed to mimic the articular cartilage.<sup>168</sup> Specifically, bone morphogenetic protein 4 and transforming growth factor- $\beta$ 3, along with mesenchymal stem cells, were encapsulated in the polymeric microsphere, poly(lactic co-glycolic acid). These cell-growth factor containing microspheres were then co-printed with the polymer, poly( $\epsilon$ -caprolactone) to form the complex structure. A similar approach can be under-

taken with nanoparticle-embedded hydrogels. With nanoparticles, it can be easier to control the mechanical properties of the articular cartilage spatiotemporally. Also, nanoparticles can contribute towards the sustained release of growth factors.<sup>169</sup> Novel nanomaterials, like metal-organic-framework nanoparticles (MOFs) should be investigated for improving growth factor delivery.<sup>170</sup> MOFs have organic/inorganic hybrid structures, and their chemistry can be easily manipulated to alter their physicochemical properties. Because of their tunable pore size/overall structure, ease of functionalization, high surface area/loading capacity, biocompatibility, and biodegradability, MOFs have found several biomedical applications.<sup>170</sup> MOFs can be bioprinted with highly tunable DNA-based polymer to synthesize drug delivery-based bioplat-forms.<sup>171</sup> Sustained release of growth factors, like bone morphogenetic protein-6, is one such application.<sup>172</sup> Therefore, the multiple benefits of nanoparticles should be exploited to prepare bioinks for mimicking the articular cartilage.

Printable hydrogel-based high-throughput drug-screening platform has recently gained momentum in pharmaceutical industry and drug development research, and nanocomposite hydrogel bioinks with their superior mechanical and tunable biological properties offer significant advantages. In fact, a high-throughput, hydrogel microarray was recently bioprinted to screen proteins that can prevent antibiotic resistance.<sup>173</sup> Enzymes, such as  $\beta$ -lactamase synthesized by bacteria, can degrade antibiotics. Proteins that inhibit these enzymes can then prevent antibiotic degradation and hinder the subsequent development of antibiotic resistance. However, some protein candidates are prone to aggregation and non-specific inhibition. Therefore, finding effective proteins that can specifically inhibit such enzymes is challenging. The hydrogel microarray developed in the study could identify proteins that can specifically inhibit  $\beta$ -lactamase.<sup>173</sup> Here, the enzyme was immobilized in a hydrogel microarray. Subsequently, the microarray was exposed to candidate protein solutions and a colorimetric substrate of  $\beta$ -lactamase. This was followed by colorimetric reading to determine the activity of the immobilized enzyme in the presence of the inhibitor proteins. Aggregated proteins were too big to enter the hydrogel matrix and interact non-specifically with the enzyme to give false-positive results. Nanocomposite hydrogels have already been shown as promising candidates for enzyme immobilization.<sup>174</sup> Therefore, similar size-exclusion, microarray-based techniques can be developed with nanoparticle incorporated hydrogels. However, care must be taken in ensuring the retention of enzyme activity after physical entrapment. Carefully designed platforms can then be used for both enzyme immobilization and high-throughput drug screening.

Other than the high-throughput enzyme-immobilization screening platforms, nanocomposite hydrogel-based bioinks can also be used for preparing *in vitro* tissue models. The designed tissues can then be used for various applications, including drug discovery through screening of target molecules and assessing those molecules' biocompatibility. Cardiac tissue models have recently been bioprinted by encapsulating

stem cell-derived cardiomyocytes in gelatin methacrylamide hydrogel.<sup>175</sup> However, cardiac tissue is electroactive, and such tissue-mimicking platforms must be electroconductive. Therefore, the addition of electroconductive nanoparticles, such as carbon nanofibers, can improve the efficacy of the *in vitro* cardiac tissue models.<sup>176</sup>

In recent years, tissue engineered scaffolds and nanocomposites have gained spotlight as a potential platform to develop physiologically representative *in vitro* models of viral disease.<sup>177–180</sup> These innovative platforms can be utilized for high-throughput screening of new small drug molecules, prophylactic and therapeutic vaccines. Such scaffolds have also been used as vaccine platforms to deliver specific antigens for stimulating the immune system.<sup>181–183</sup> Nanoengineered bioinks and additive manufacturing technologies can provide rare set of tools that can facilitate printing complex scaffold structures with high precision for vaccine research.

## 6. Conclusion

To conclude, in this review paper, we took a material-centric approach and aimed to illustrate how nanoparticle-reinforced polymeric hydrogels can synergistically improve mechanical, biological, functional, and printable properties of traditional bioink hydrogels and harness their properties for various clinically relevant tissue engineering applications. We discussed the unique functionalities brought about by nanoparticle-polymer interactions that create the highly functional, external-stimuli responsive, smart nanocomposite hydrogels. Uncovering the fundamental rules that govern such nanoparticle-polymer interactions in diverse nanocomposite bioink hydrogels may also have broad and significant implications in designing the future generations of bioprinters for additive manufacturing.

## Conflicts of interest

Authors declare no conflict of interest.

## Acknowledgements

A. P. is grateful for the funding and support from Canada Research Chairs Program of the Natural Sciences and Engineering Research Council (NSERC) of Canada, NSERC Discovery grant, NSERC Discovery Accelerator Supplements (DAS), New Frontiers in Research Fund (NFRF)- Exploration Stream, Early Research Award (ERA) from Province of Ontario, The Center for Advanced Materials and Biomaterials Research (CAMBR) Seed Grant, Western Strategic Support-CIHR Seed Grant, and Wolfe-Western Fellowship At-Large for Outstanding Newly Recruited Research Scholar. The authors would also like to acknowledge the company, Biorender. Some of the images were created with Biorender.com.

## References

- 1 S. V. Murphy and A. Atala, *Nat. Biotechnol.*, 2014, **32**, 773–785.
- 2 M. Singh and S. Jonnalagadda, *Eur. J. Pharm. Sci.*, 2020, **143**, 105167.
- 3 M. Askari, M. Afzali Naniz, M. Kouhi, A. Saberi, A. Zolfagharian and M. Bodaghi, *Biomater. Sci.*, 2021, **9**, 535–573.
- 4 N. Khoshnood and A. Zamanian, *Bioprinting*, 2020, **19**, e00088.
- 5 Y. Wu, D. J. Ravnic and I. T. Ozbolat, *Trends Biotechnol.*, 2020, **38**, 594–605.
- 6 J. Gopinathan and I. Noh, *Biomater. Res.*, 2018, **22**, 1–15.
- 7 J. Groll, J. A. Burdick, D. W. Cho, B. Derby, M. Gelinsky, S. C. Heilshorn, T. Jüngst, J. Malda, V. A. Mironov, K. Nakayama, A. Ovsianikov, W. Sun, S. Takeuchi, J. J. Yoo and T. B. F. Woodfield, *Biofabrication*, 2019, **11**, 013001.
- 8 P. S. Gungor-Ozkerim, I. Inci, Y. S. Zhang, A. Khademhosseini and M. R. Dokmeci, *Biomater. Sci.*, 2018, **6**, 915–946.
- 9 W. Zhu, H. Cui, B. Boualam, F. Masood, E. Flynn, R. D. Rao, Z.-Y. Zhang and L. G. Zhang, *Nanotechnology*, 2018, **29**, 185101.
- 10 T. Gonzalez-Fernandez, S. Rathan, C. Hobbs, P. Pitacco, F. E. Freeman, G. M. Cunniffe, N. J. Dunne, H. O. McCarthy, V. Nicolosi, F. J. O'Brien and D. J. Kelly, *J. Controlled Release*, 2019, **301**, 13–27.
- 11 I. Donderwinkel, J. C. M. van Hest and N. R. Cameron, *Polym. Chem.*, 2017, **8**, 4451–4471.
- 12 T. T. Demirtaş, G. Irmak and M. Gümüşderelioglu, *Biofabrication*, 2017, **9**, 035003.
- 13 B. B. Mendes, M. Gómez-Florit, A. G. Hamilton, M. S. Detamore, R. M. A. Domingues, R. L. Reis and M. E. Gomes, *Biofabrication*, 2019, **12**, 015012.
- 14 K. Y. Lee and D. J. Mooney, *Chem. Rev.*, 2001, **101**, 1869–1879.
- 15 Y. Guo, J. Bae, Z. Fang, P. Li, F. Zhao and G. Yu, *Chem. Rev.*, 2020, **120**, 7642–7707.
- 16 E. M. Ahmed, *J. Adv. Res.*, 2015, **6**, 105–121.
- 17 A. S. Hoffman, *Adv. Drug Delivery Rev.*, 2012, **64**, 18–23.
- 18 V. G. Muir and J. A. Burdick, *Chem. Rev.*, 2021, DOI: 10.1021/acs.chemrev.0c00923.
- 19 E. Mancha Sánchez, J. C. Gómez-Blanco, E. López Nieto, J. G. Casado, A. Macías-García, M. A. Díaz Díez, J. P. Carrasco-Amador, D. Torrejón Martín, F. M. Sánchez-Margallo and J. B. Pagador, *Front. Bioeng. Biotechnol.*, 2020, **8**, 776.
- 20 Z. Bao, C. Xian, Q. Yuan, G. Liu and J. Wu, *Adv. Healthcare Mater.*, 2019, **8**, 1900670.
- 21 R. Kuijjer, E. J. P. Jansen, P. J. Emans, S. K. Bulstra, J. Riesle, J. Pieper, D. W. Grainger and H. J. Busscher, *Biomaterials*, 2007, **28**, 5148–5154.
- 22 Q. Chen, H. Chen, L. Zhu and J. Zheng, *J. Mater. Chem. B*, 2015, **3**, 3654–3676.
- 23 P. A. Panteli, C. S. Patrickios, M. Constantinou and G. Constantinides, *Macromol. Symp.*, 2019, **385**, 1800201.

- 24 X. Wang, Z. Li, T. Shi, P. Zhao, K. An, C. Lin and H. Liu, *Mater. Sci. Eng. C*, 2017, **73**, 21–30.
- 25 X. Dou, N. Mehwish, C. Zhao, J. Liu, C. Xing and C. Feng, *Acc. Chem. Res.*, 2020, **53**, 852–862.
- 26 A. Bhattacharyya, G. Janarthanan, H. N. Tran, H. J. Ham, J. H. Yoon and I. Noh, *Chem. Eng. J.*, 2021, **415**, 128971.
- 27 X. Cui, J. Li, Y. Hartanto, M. Durham, J. Tang, H. Zhang, G. Hooper, K. Lim and T. Woodfield, *Adv. Healthcare Mater.*, 2020, **9**, 1901648.
- 28 A. K. Gaharwar, N. A. Peppas and A. Khademhosseini, *Biotechnol. Bioeng.*, 2014, **111**, 441–453.
- 29 M. Yang, Z. Yuan, J. Liu, Z. Fang, L. Fang, D. Yu and Q. Li, *Adv. Opt. Mater.*, 2019, **7**, 1900069.
- 30 R. Tognato, A. R. Armiento, V. Bonfrate, R. Levato, J. Malda, M. Alini, D. Eglin, G. Giancane and T. Serra, *Adv. Funct. Mater.*, 2019, **29**, 1804647.
- 31 M. Mihajlovic, M. Mihajlovic, P. Y. W. Dankers, R. Masereeuw and R. P. Sijbesma, *Macromol. Biosci.*, 2019, **19**, 1800173.
- 32 C. Shen, Y. Zhao, H. Liu, Y. Jiang, H. Li, S. Lan, H. Bao, B. Yang and Q. Lin, *Polym. Chem.*, 2018, **9**, 2478–2483.
- 33 A. M. Brokesh and A. K. Gaharwar, *ACS Appl. Mater. Interfaces*, 2020, **12**, 5319–5344.
- 34 A. Paul, V. Manoharan, D. Krafft, A. Assmann, J. A. Uquillas, S. R. Shin, A. Hasan, M. A. Hussain, A. Memic, A. K. Gaharwar and A. Khademhosseini, *J. Mater. Chem. B*, 2016, **4**, 3544–3554.
- 35 S. Basu, S. Pacelli, Y. Feng, Q. Lu, J. Wang and A. Paul, *ACS Nano*, 2018, **12**, 9866–9880.
- 36 S. Basu, S. Pacelli and A. Paul, *Acta Biomater.*, 2020, **105**, 159–169.
- 37 A. J. Clasky, J. D. Watchorn, P. Z. Chen and F. X. Gu, *Acta Biomater.*, 2021, **122**, 1–25.
- 38 K. Varaprasad, Y. M. Mohan, S. Ravindra, N. N. Reddy, K. Vimala, K. Monika, B. Sreedhar and K. M. Raju, *J. Appl. Polym. Sci.*, 2010, **115**, 1199–1207.
- 39 T. Yata, Y. Takahashi, M. Tan, H. Nakatsuji, S. Ohtsuki, T. Murakami, H. Imahori, Y. Umeki, T. Shiomi, Y. Takakura and M. Nishikawa, *Biomaterials*, 2017, **146**, 136–145.
- 40 D. Chimene, C. W. Peak, J. L. Gentry, J. K. Carrow, L. M. Cross, E. Mondragon, G. B. Cardoso, R. Kaunas and A. K. Gaharwar, *ACS Appl. Mater. Interfaces*, 2018, **10**, 9957–9968.
- 41 Y. Jin, Y. Shen, J. Yin, J. Qian and Y. Huang, *ACS Appl. Mater. Interfaces*, 2018, **10**, 10461–10470.
- 42 S. Pacelli, R. Maloney, A. R. Chakravarti, J. Whitlow, S. Basu, S. Modaresi, S. Gehrke and A. Paul, *Sci. Rep.*, 2017, **7**, 1–15.
- 43 H. Wu, L. Song, L. Chen, Y. Huang, Y. Wu, F. Zang, Y. An, H. Lyu, M. Ma, J. Chen, N. Gu and Y. Zhang, *Nanoscale*, 2017, **9**, 16175–16182.
- 44 Y. W. Jiang, G. Gao, P. Hu, J. B. Liu, Y. Guo, X. Zhang, X. W. Yu, F. G. Wu and X. Lu, *Nanoscale*, 2020, **12**, 210–219.
- 45 D. Williams, P. Thayer, H. Martinez, E. Gatenholm and A. Khademhosseini, *Bioprinting*, 2018, **9**, 19–36.
- 46 L. Ouyang, C. B. Highley, W. Sun and J. A. Burdick, *Adv. Mater.*, 2017, **29**, 1604983.
- 47 J. H. Galarraga, M. Y. Kwon and J. A. Burdick, *Sci. Rep.*, 2019, **9**, 1–12.
- 48 L. Ning, N. Zhu, F. Mohabatpour, M. D. Sarker, D. J. Schreyer and X. Chen, *J. Mater. Chem. B*, 2019, **7**, 4538–4551.
- 49 D. Chimene, R. Kaunas and A. K. Gaharwar, *Adv. Mater.*, 2020, **32**, 1902026.
- 50 J. Li, J. Ma, S. Chen, Y. Huang and J. He, *Mater. Sci. Eng. C*, 2018, **89**, 25–32.
- 51 A. Kumar, I. A. I. Matari, H. Choi, A. Kim, Y. J. Suk, J. Y. Kim and S. S. Han, *Mater. Sci. Eng. C*, 2019, **104**, 109983.
- 52 X. Yang, S. K. Biswas, H. Yano and K. Abe, *Cellulose*, 2020, **27**, 693–702.
- 53 C. Shao, M. Wang, H. Chang, F. Xu and J. Yang, *ACS Sustainable Chem. Eng.*, 2017, **5**, 6167–6174.
- 54 Y. Wang, G. Xiao, Y. Peng, L. Chen and S. Fu, *Cellulose*, 2019, **26**, 8813–8827.
- 55 D. L. Taylor and M. in het Panhuis, *Adv. Mater.*, 2016, **28**, 9060–9093.
- 56 A. K. Gaharwar, R. K. Avery, A. Assmann, A. Paul, G. H. McKinley, A. Khademhosseini and B. D. Olsen, *ACS Nano*, 2014, **8**, 9833–9842.
- 57 K. Phogat, S. Kanwar, D. Nayak, N. Mathur, S. B. Ghosh and S. Bandyopadhyay-Ghosh, *J. Appl. Polym. Sci.*, 2020, **137**, 48789.
- 58 M. Guvendiren, H. D. Lu and J. A. Burdick, *Soft Matter*, 2011, **8**, 260–272.
- 59 A. Perazzo, J. K. Nunes, S. Guido and H. A. Stone, *PNAS*, 2017, **114**, E8557–E8564.
- 60 X. Li, B. Liu, B. Pei, J. Chen, D. Zhou, J. Peng, X. Zhang, W. Jia and T. Xu, *Chem. Rev.*, 2020, **120**, 10793–10833.
- 61 N. Paxton, W. Smolan, T. Böck, F. Melchels, J. Groll and T. Jungst, *Biofabrication*, 2017, **9**, 044107.
- 62 L. Wei, Z. Li, J. Li, Y. Zhang, B. Yao, Y. Liu, W. Song, X. Fu, X. Wu and S. Huang, *J. Mater. Sci.: Mater. Med.*, 2020, **31**, 1–12.
- 63 S. Catros, J.-C. Fricain, B. Guillotin, B. Pippenger, R. Bareille, M. Remy, E. Lebraud, B. Desbat, J. Amédée and F. Guillemot, *Biofabrication*, 2011, **3**, 025001.
- 64 G. Gao, A. F. Schilling, T. Yonezawa, J. Wang, G. Dai and X. Cui, *Biotechnol. J.*, 2014, **9**, 1304–1311.
- 65 N. J. Castro, J. O'Brien and L. G. Zhang, *Nanoscale*, 2015, **7**, 14010–14022.
- 66 J. Adhikari, A. Roy, A. Das, M. Ghosh, S. Thomas, A. Sinha, J. Kim and P. Saha, *Macromol. Biosci.*, 2021, **21**, 2000179.
- 67 P. Datta, A. Barui, Y. Wu, V. Ozbolat, K. K. Moncal and I. T. Ozbolat, *Biotechnol. Adv.*, 2018, **36**, 1481–1504.
- 68 A. Blaeser, D. Filipa Duarte Campos, U. Puster, W. Richtering, M. M. Stevens and H. Fischer, *Adv. Healthcare Mater.*, 2016, **5**, 326–333.
- 69 S. Derakhshanfar, R. Mbeleck, K. Xu, X. Zhang, W. Zhong and M. Xing, *Bioact. Mater.*, 2018, **3**, 144–156.

- 70 W. Bao, M. Li, Y. Yang, Y. Wan, X. Wang, N. Bi and C. Li, *Front. Chem.*, 2020, **8**, 53.
- 71 N. Asadi, E. Alizadeh, R. Salehi, B. Khalandi, S. Davaran and A. Akbarzadeh, *Artif. Cells, Nanomed., Biotechnol.*, 2018, **46**, 465–471.
- 72 T. Ahlfeld, G. Cidonio, D. Kilian, S. Duin, A. R. Akkineni, J. I. Dawson, S. Yang, A. Lode, R. O. C. Oreffo and M. Gelinsky, *Biofabrication*, 2017, **9**, 034103.
- 73 H. Li, S. Liu and L. Li, *Int. J. Bioprint.*, 2016, **2**, 54–66.
- 74 M. Izadifar, D. Chapman, P. Babyn, X. Chen and M. E. Kelly, *Tissue Eng., Part C*, 2018, **24**, 74–88.
- 75 Cellulose Nanofibers for the Enhancement of Printability of Low Viscosity Gelatin Derivatives | Shin | BioResources, <https://ojs.cnr.ncsu.edu/index.php/BioRes/article/view/11043>, (accessed April 15, 2021).
- 76 M. T. Tavares, V. M. Gaspar, M. V. Monteiro, J. P. S. Farinha, C. Baleizao and J. Mano, *Biofabrication*, 2021, **13**, 035012.
- 77 J. Li, Y. Zhang, J. Enhe, B. Yao, Y. Wang, D. Zhu, Z. Li, W. Song, X. Duan, X. Yuan, X. Fu and S. Huang, *Mater. Sci. Eng., C*, 2021, **126**, 112193.
- 78 L. Kuang, X. Ma, Y. Ma, Y. Yao, M. Tariq, Y. Yuan and C. Liu, *ACS Appl. Mater. Interfaces*, 2019, **11**, 17234–17246.
- 79 F. E. Freeman, P. Pitacco, L. H. A. van Dommelen, J. Nulty, D. C. Browe, J. Y. Shin, E. Alsberg and D. J. Kelly, *Sci. Adv.*, 2020, **6**, 5093–5107.
- 80 C. Hu, L. Hahn, M. Yang, A. Altmann, P. Stahlhut, J. Groll and R. Luxenhofer, *J. Mater. Sci.*, 2021, **56**, 691–705.
- 81 Y. Guo, J. A. Belgodere, Y. Ma, J. P. Jung and B. Bharti, *Macromol. Rapid Commun.*, 2019, **40**, 1900191.
- 82 X. Zhang, C. L. Pint, M. H. Lee, B. E. Schubert, A. Jamshidi, K. Takei, H. Ko, A. Gillies, R. Bardhan, J. J. Urban, M. Wu, R. Fearing and A. Javey, *Nano Lett.*, 2011, **11**, 3239–3244.
- 83 L. Wu, J. Virdee, E. Maughan, A. Darbyshire, G. Jell, M. Loizidou, M. Emberton, P. Butler, A. Howkins, A. Reynolds, I. W. Boyd, M. Birchall and W. Song, *Acta Biomater.*, 2018, **80**, 188–202.
- 84 S. Fu, G. Guo, C. Gong, S. Zeng, H. Liang, F. Luo, X. Zhang, X. Zhao, Y. Wei and Z. Qian, *J. Phys. Chem. B*, 2009, **113**, 16518–16525.
- 85 S. A. Wilson, L. M. Cross, C. W. Peak and A. K. Gaharwar, *ACS Appl. Mater. Interfaces*, 2017, **9**, 43449–43458.
- 86 K. Srinivasan and R. Mahadevan, *BMC Biotechnol.*, 2010, **10**, 2.
- 87 X. Hu, Z. Gao, H. Tan, H. Wang, X. Mao and J. Pang, *Front. Chem.*, 2019, 477.
- 88 S. Wei, X. Liu, J. Zhou, J. Zhang, A. Dong, P. Huang, W. Wang and L. Deng, *Int. J. Biol. Macromol.*, 2020, **155**, 153–162.
- 89 C. Wu, J. Liu, Z. Zhai, L. Yang, X. Tang, L. Zhao, K. Xu and W. Zhong, *Acta Biomater.*, 2020, **106**, 278–288.
- 90 M. Wu, J. Chen, W. Huang, B. Yan, Q. Peng, J. Liu, L. Chen and H. Zeng, *Biomacromolecules*, 2020, **21**, 2409–2420.
- 91 D. G. Lim, E. Kang and S. H. Jeong, *J. Nanobiotechnol.*, 2020, **18**, 88.
- 92 S. R. Shin, H. Bae, J. M. Cha, J. Y. Mun, Y. C. Chen, H. Tekin, H. Shin, S. Farshchi, M. R. Dokmeci, S. Tang and A. Khademhosseini, *ACS Nano*, 2012, **6**, 362–372.
- 93 A. Nadernezhad, N. Khani and B. Koc, *Procedia CIRP*, 2017, **65**, 44–47.
- 94 J. He, M. Shi, Y. Liang and B. Guo, *Chem. Eng. J.*, 2020, **394**, 124888.
- 95 C. T. Huang, L. Kumar Shrestha, K. Ariga and S. H. Hsu, *J. Mater. Chem. B*, 2017, **5**, 8854–8864.
- 96 K. Zhu, S. R. Shin, T. van Kempen, Y.-C. Li, V. Ponraj, A. Nasajpour, S. Mandla, N. Hu, X. Liu, J. Leijten, Y.-D. Lin, M. A. Hussain, Y. S. Zhang, A. Tamayol and A. Khademhosseini, *Adv. Funct. Mater.*, 2017, **27**, 1605352.
- 97 W. Kim, C. H. Jang and G. H. Kim, *Nano Lett.*, 2019, **19**, 8612–8620.
- 98 S.-J. Lee, T. Esworthy, S. Stake, S. Miao, Y. Y. Zuo, B. T. Harris and L. G. Zhang, *Adv. Biosyst.*, 2018, **2**, 1700213.
- 99 H. Budharaju, A. Subramanian and S. Sethuraman, *Biomater. Sci.*, 2021, **9**, 1974–1994.
- 100 S. R. Shin, S. M. Jung, M. Zalabany, K. Kim, P. Zorlutuna, S. B. Kim, M. Nikkhah, M. Khabiry, M. Azize, J. Kong, K. T. Wan, T. Palacios, M. R. Dokmeci, H. Bae, X. Tang and A. Khademhosseini, *ACS Nano*, 2013, **7**, 2369–2380.
- 101 S. Pok, F. Vitale, S. L. Eichmann, O. M. Benavides, M. Pasquali and J. G. Jacot, *ACS Nano*, 2014, **8**, 9822–9832.
- 102 M. Kharaziha, S. R. Shin, M. Nikkhah, S. N. Topkaya, N. Masoumi, N. Annabi, M. R. Dokmeci and A. Khademhosseini, *Biomaterials*, 2014, **35**, 7346–7354.
- 103 S. R. Shin, R. Farzad, A. Tamayol, V. Manoharan, P. Mostafalu, Y. S. Zhang, M. Akbari, S. M. Jung, D. Kim, M. Comotto, N. Annabi, F. E. Al-Hazmi, M. R. Dokmeci and A. Khademhosseini, *Adv. Mater.*, 2016, **28**, 3280–3289.
- 104 S. Jain, S. R. Singh and S. Pillai, DOI: 10.4172/2157-7439.1000140.
- 105 H. Dumortier, *Adv. Drug Delivery Rev.*, 2013, **65**, 2120–2126.
- 106 S. Vardharajula, Sk. Z. Ali, P. M. Tiwari, E. Eroğlu, K. Vig, V. A. Dennis and S. R. Singh, *Int. J. Nanomed.*, 2012, **7**, 5361–5374.
- 107 A. Motealleh and N. S. Kehr, *Adv. Healthcare Mater.*, 2017, **6**, 1600938.
- 108 C. Fasciani, M. J. Silvero, M. A. Anghel, G. A. Argüello, M. C. Becerra and J. C. Scaiano, *J. Am. Chem. Soc.*, 2014, **136**, 17394–17397.
- 109 S. W. Lv, Y. Liu, M. Xie, J. Wang, X. W. Yan, Z. Li, W. G. Dong and W. H. Huang, *ACS Nano*, 2016, **10**, 6201–6210.
- 110 B. Yan, J. C. Boyer, D. Habault, N. R. Branda and Y. Zhao, *J. Am. Chem. Soc.*, 2012, **134**, 16558–16561.
- 111 B. Xia, W. Zhang, H. Tong, J. Li, Z. Chen and J. Shi, *ACS Biomater. Sci. Eng.*, 2019, **5**, 1857–1867.
- 112 Z. Deng, T. Hu, Q. Lei, J. He, P. X. Ma and B. Guo, *ACS Appl. Mater. Interfaces*, 2019, **11**, 6796–6808.
- 113 N. Yang, M. Zhu, G. Xu, N. Liu and C. Yu, *J. Mater. Chem. B*, 2020, **8**, 3908–3917.



- 114 X. Yang, L. Gao, Q. Guo, Y. Li, Y. Ma, J. Yang, C. Gong and C. Yi, *Nano Res.*, 2020, **13**, 2579–2594.
- 115 J. Zeng, D. Shi, Y. Gu, T. Kaneko, L. Zhang, H. Zhang, D. Kaneko and M. Chen, *Biomacromolecules*, 2019, **20**, 3375–3384.
- 116 Y. Li, G. Huang, X. Zhang, B. Li, Y. Chen, T. Lu, T. J. Lu and F. Xu, *Adv. Funct. Mater.*, 2013, **23**, 660–672.
- 117 M. Betsch, C. Cristian, Y.-Y. Lin, A. Blaeser, J. Schöneberg, M. Vogt, E. M. Buhl, H. Fischer and D. F. D. Campos, *Adv. Healthcare Mater.*, 2018, **7**, 1800894.
- 118 D. Podstawczyk, M. Nizioł, P. Szymczyk, P. Wiśniewski and A. Guiseppi-Elie, *Addit. Manuf.*, 2020, **34**, 101275.
- 119 L.-M. Lacroix, J. Carrey and M. Respaud, *Rev. Sci. Instrum.*, 2008, **79**, 093909.
- 120 J. Zhang, S. Zhao, M. Zhu, Y. Zhu, Y. Zhang, Z. Liu and C. Zhang, *J. Mater. Chem. B*, 2014, **2**, 7583–7595.
- 121 J. I. Kim, C. J. Chun, B. Kim, J. M. Hong, J. K. Cho, S. H. Lee and S. C. Song, *Biomaterials*, 2012, **33**, 218–224.
- 122 C. J. Sunderland, M. Steiert, J. E. Talmadge, A. M. Derfus and S. E. Barry, *Drug Dev. Res.*, 2006, **67**, 70–93.
- 123 H. Tseng, J. A. Gage, T. Shen, W. L. Haisler, S. K. Neeley, S. Shiao, J. Chen, P. K. Desai, A. Liao, C. Hebel, R. M. Raphael, J. L. Becker and G. R. Souza, *Sci. Rep.*, 2015, **5**, 1–11.
- 124 V. A. Parfenov, Y. D. Khesuani, S. V. Petrov, P. A. Karalkin, E. V. Koudan, E. K. Nezhurina, F. D. A. S. Pereira, A. A. Krokmal, A. A. Gryadunova, E. A. Bulanova, I. V. Vakhrushev, I. I. Babichenko, V. Kasyanov, O. F. Petrov, M. M. Vasiliev, K. Brakke, S. I. Belousov, T. E. Grigoriev, E. O. Osidak, E. I. Rossiyskaya, L. B. Buravkova, O. D. Kononenko, U. Demirci and V. A. Mironov, *Sci. Adv.*, 2020, **6**, eaba4174.
- 125 R. V. Ramanujan and L. L. Lao, *Smart Mater. Struct.*, 2006, **15**, 952–956.
- 126 Z. Hooshyar and G. R. Bardajee, *J. Iran. Chem. Soc.*, 2017, **14**, 541–549.
- 127 X. Xu, Z. Huang, Z. Huang, X. Zhang, S. He, X. Sun, Y. Shen, M. Yan and C. Zhao, *ACS Appl. Mater. Interfaces*, 2017, **9**, 20361–20375.
- 128 A. Augurio, P. Cortelletti, R. Tognato, A. Rios, R. Levato, J. Malda, M. Alini, D. Eglin, G. Giancane, A. Speghini and T. Serra, *Adv. Intell. Syst.*, 2020, **2**, 1900105.
- 129 Y. Chen, J. Zhang, X. Liu, S. Wang, J. Tao, Y. Huang, W. Wu, Y. Li, K. Zhou, X. Wei, X. Wei, S. Chen, X. Li, X. Xu, L. Cardon, Z. Qian and M. Gou, *Sci. Adv.*, 2020, **6**, eaba7406.
- 130 H. Palza, *Int. J. Mol. Sci.*, 2015, **16**, 2099–2116.
- 131 B. W. Walker, R. P. Lara, E. Mogadam, C. H. Yu, W. Kimball and N. Annabi, *Prog. Polym. Sci.*, 2019, **92**, 135–157.
- 132 A. A. Adedoyin and A. K. Ekenseair, *Nano Res.*, 2018, **11**, 5049–5064.
- 133 B. Lin, J. Wu, Y. Wang, S. Sun, Y. Yuan, X. Tao and R. Lv, *Biomater. Sci.*, 2021, **9**, 1000–1007.
- 134 X. Li, W. Zhang, J. Lin, H. Wu, Y. Yao, J. Zhang and C. Yang, *Biomater. Sci.*, 2021, **9**, 3453–3464.
- 135 M. Ajdary, M. Moosavi, M. Rahmati, M. Falahati, M. Mahboubi, A. Mandegary, S. Jangjoo, R. Mohammadinejad and R. Varma, *Nanomaterials*, 2018, **8**, 634.
- 136 M. Akter, M. T. Sikder, M. M. Rahman, A. K. M. A. Ullah, K. F. B. Hossain, S. Banik, T. Hosokawa, T. Saito and M. Kurasaki, *J. Adv. Res.*, 2018, **9**, 1–16.
- 137 Z. Yu, Q. Li, J. Wang, Y. Yu, Y. Wang, Q. Zhou and P. Li, *Nanoscale Res. Lett.*, 2020, **15**, 1–14.
- 138 A. L. Silva, C. Peres, J. Coniot, A. I. Matos, L. Moura, B. Carreira, V. Sainz, A. Scomparin, R. Satchi-Fainaro, V. Pr eat and H. F. Florindo, *Semin. Immunol.*, 2017, **34**, 3–24.
- 139 G. Qu, W. Liu, Y. Zhao, J. Gao, T. Xia, J. Shi, L. Hu, W. Zhou, J. Gao, H. Wang, Q. Luo, Q. Zhou, S. Liu, X.-F. Yu and G. Jiang, *Angew. Chem., Int. Ed.*, 2017, **56**, 14488–14493.
- 140 H. Rastin, B. Zhang, A. Mazinani, K. Hassan, J. Bi, T. T. Tung and D. Losic, *Nanoscale*, 2020, **12**, 16069–16080.
- 141 A. Nadernezhad, O. S. Caliskan, F. Topuz, F. Afghah, B. Erman and B. Koc, *ACS Appl. Bio Mater.*, 2019, **2**, 796–806.
- 142 Y. Zhang, Y. Yu, A. Akkouch, A. Dababneh, F. Dolati and I. T. Ozbolat, *Biomater. Sci.*, 2015, **3**, 134–143.
- 143 M. L. Bedell, A. J. Melchiorri, J. Aleman, A. Skardal and A. G. Mikos, *Bioprinting*, 2020, **17**, e00068.
- 144 D. Septiadi, F. Crippa, T. L. Moore, B. Rothen-Rutishauser and A. Petri-Fink, *Adv. Mater.*, 2018, **30**, 1704463.
- 145 S. Barillet, E. Fattal, S. Mura, N. Tsapis, M. Pallardy, H. Hillaireau and S. Kerdine-R omer, *Nanotoxicology*, 2019, **13**, 606–622.
- 146 S. Heid and A. R. Boccaccini, *Acta Biomater.*, 2020, **113**, 1–22.
- 147 A. Bhattacharyya, G. Janarthanan and I. Noh, *Addit. Manuf.*, 2021, **37**, 101639.
- 148 J. Adhikari, M. S. Perwez, A. Das and P. Saha, *Nano-Struct. Nano-Objects*, 2021, **25**, 100630.
- 149 M. Lee, K. Bae, P. Guillon, J. Chang,  . Arlov and M. Zenobi-Wong, *ACS Appl. Mater. Interfaces*, 2018, **10**, 37820–37828.
- 150 C. Murphy, K. Kolan, W. Li, J. Semon, D. Day and M. Leu, *Int. J. Bioprint.*, 2017, **3**, 53–63.
- 151 G. Cidonio, C. R. Alcal -Orozco, K. S. Lim, M. Glinka, I. Mutreja, Y. H. Kim, J. I. Dawson, T. B. F. Woodfield and R. O. C. Oreffo, *Biofabrication*, 2019, **11**, 035027.
- 152 X. Sun, Z. Ma, X. Zhao, W. Jin, C. Zhang, J. Ma, L. Qiang, W. Wang, Q. Deng, H. Yang, J. Zhao, Q. Liang, X. Zhou, T. Li and J. Wang, *Bioact. Mater.*, 2021, **6**, 757–769.
- 153 J. Wu, C. Qin, J. Ma, H. Zhang, J. Chang, L. Mao and C. Wu, *Appl. Mater. Today*, 2021, **23**, 101015.
- 154 S. Vijayavenkataraman, W. C. Yan, W. F. Lu, C. H. Wang and J. Y. H. Fuh, *Adv. Drug Delivery Rev.*, 2018, **132**, 296–332.
- 155 P. Abdollahiyan, F. Oroojalian, A. Mokhtarzadeh and M. Guardia, *Biotechnol. J.*, 2020, **15**, 2000095.

- 156 C. C. Piras and D. K. Smith, *J. Mater. Chem. B*, 2020, **8**, 8171–8188.
- 157 X. Chen, Z. Yue, P. C. Winberg, Y.-R. Lou, S. Beirne and G. G. Wallace, *Biomater. Sci.*, 2021, **9**, 2424–2438.
- 158 S. Kumar, A. Tharayil and S. Thomas, *ACS Appl. Polym. Mater.*, 2021, DOI: 10.1021/acspam.1c00567.
- 159 G. Choe, S. Oh, J. M. Seok, S. A. Park and J. Y. Lee, *Nanoscale*, 2019, **11**, 23275–23285.
- 160 M. K. Jaiswal, J. R. Xavier, J. K. Carrow, P. Desai, D. Alge and A. K. Gaharwar, *ACS Nano*, 2016, **10**, 246–256.
- 161 Y. Yong, L. Zhou, Z. Gu, L. Yan, G. Tian, X. Zheng, X. Liu, X. Zhang, J. Shi, W. Cong, W. Yin and Y. Zhao, *Nanoscale*, 2014, **6**, 10394–10403.
- 162 X. Chen and A. R. McDonald, *Adv. Mater.*, 2016, **28**, 5738–5746.
- 163 M. K. Jaiswal, J. K. Carrow, J. L. Gentry, J. Gupta, N. Altangerel, M. Scully and A. K. Gaharwar, *Adv. Mater.*, 2017, **29**, 1702037.
- 164 N. Zandi, E. S. Sani, E. Mostafavi, D. M. Ibrahim, B. Saleh, M. A. Shokrgozar, E. Tamjid, P. S. Weiss, A. Simchi and N. Annabi, *Biomaterials*, 2021, **267**, 120476.
- 165 M. Albanna, K. W. Binder, S. V. Murphy, J. Kim, S. A. Qasem, W. Zhao, J. Tan, I. B. El-Amin, D. D. Dice, J. Marco, J. Green, T. Xu, A. Skardal, J. H. Holmes, J. D. Jackson, A. Atala and J. J. Yoo, *Sci. Rep.*, 2019, **9**, 1–15.
- 166 H. Ding and R. C. Chang, *Addit. Manuf.*, 2018, **22**, 708–719.
- 167 A. J. S. Fox, A. Bedi and S. A. Rodeo, *Sports Health*, 2009, **1**, 461–468.
- 168 Y. Sun, Y. You, W. Jiang, B. Wang, Q. Wu and K. Dai, *Sci. Adv.*, 2020, **6**, eaay1422.
- 169 Z. Wang, Z. Wang, W. W. Lu, W. Zhen, D. Yang and S. Peng, *NPG Asia Mater.*, 2017, **9**, e435.
- 170 J. Yang and Y. Yang, *Small*, 2020, **16**, 1906846.
- 171 A. Chakraborty, S. P. Ravi, Y. Shamiya, C. Cui and A. Paul, *Chem. Soc. Rev.*, 2021, **50**, 7779–7819.
- 172 Ö. Toprak, B. Topuz, Y. A. Monsef, Ç. Oto, K. Orhan and A. Karakeçili, *Mater. Sci. Eng. C*, 2021, **120**, 111738.
- 173 R. Mateen, M. M. Ali and T. Hoare, *Nat. Commun.*, 2018, **9**, 1–9.
- 174 J. H. Kim, S. Park, H. Kim, H. J. Kim, Y. H. Yang, Y. H. Kim, S. K. Jung, E. Kan and S. H. Lee, *Carbohydr. Polym.*, 2017, **157**, 137–145.
- 175 J. Liu, J. He, J. Liu, X. Ma, Q. Chen, N. Lawrence, W. Zhu, Y. Xu and S. Chen, *Bioprinting*, 2019, **13**, e00040.
- 176 A. M. Martins, G. Eng, S. G. Caridade, J. F. Mano, R. L. Reis and G. Vunjak-Novakovic, *Biomacromolecules*, 2014, **15**, 635–643.
- 177 R. Bhowmick, T. Derakhshan, Y. Liang, J. Ritchey, L. Liu and H. Gappa-Fahlenkamp, *Tissue Eng., Part A*, 2018, **24**, 1468–1480.
- 178 J. Gardner and M. Herbst-Kralovetz, *Viruses*, 2016, **8**, 304.
- 179 T. Y. Ling, M. der Kuo, C. L. Li, A. L. Yu, Y. H. Huang, T. J. Wu, Y. C. Lin, S. H. Chen and J. Yu, *Proc. Natl. Acad. Sci. U. S. A.*, 2006, **103**, 9530–9535.
- 180 A. M. Tatara, *Tissue Eng., Part A*, 2020, **26**, 468–474.
- 181 D. Sanchez-Guzman, P. le Guen, B. Villeret, N. Sola, R. le Borgne, A. Guyard, A. Kemmel, B. Crestani, J. M. Sallenave and I. Garcia-Verdugo, *Biomaterials*, 2019, **217**, 119308.
- 182 M. O. Dellacherie, A. Li, B. Y. Lu, C. S. Verbeke, L. Gu, A. G. Stafford, E. J. Doherty and D. J. Mooney, *Adv. Funct. Mater.*, 2020, **30**, 2002448.
- 183 H. Wang, A. J. Najibi, M. C. Sobral, B. R. Seo, J. Y. Lee, D. Wu, A. W. Li, C. S. Verbeke and D. J. Mooney, *Nat. Commun.*, 2020, **11**, 1–14.
- 184 N. Yang, M. Zhu, G. Xu, N. Liu and C. Yu, *J. Mater. Chem. B*, 2020, **8**, 3908–3917.